Zootaxa 4890 (1): 001–037
https://www.mapress.com/j/zt/

Article

ISSN 1175-5326 (print edition)
ZOOTAXA
ISSN 1175-5334 (online edition)

https://doi.org/10.11646/zootaxa.4890.1.1
http://zoobank.org/urn:lsid:zoobank.org:pub:C484D4D4-199E-45A0-9A38-0F6DEE3EE564

A tale of two genera: the revival of *Hoplodoris* (Nudibranchia: Discodorididae) with the description of new species of *Hoplodoris* and *Asteronotus*

SAMANTHA A. DONOHOO[1,2*] & TERRENCE M. GOSLINER[1,3]
[1]*Department of Invertebrate Zoology and Geology, California Academy of Sciences, San Francisco, CA 94118, U.S.A.*
[2]*Department of Biology, San Francisco State University, San Francisco, CA 94132, U.S.A.*
[3] *https://orcid.org/0000-0002-3950-0243*
[*]*Corresponding author.* *Sdonohoo@calacademy.org;* *https://orcid.org/0000-0002-2786-8470*

Abstract

Nudibranchs in the family Discodorididae are generally medium (~30mm) to large (> 50mm) in size, sometimes cryptic, and are found in almost every marine ecosystem around the world. The diversity and systematics of the genera within Discodorididae are poorly understood and have led to numerous taxonomic changes. *Hoplodoris* Bergh, 1880 has recently been considered a synonym of *Asteronotus* Ehrenberg, 1831; however, morphological and molecular phylogenetic analyses reveal a distinct separation between these two genera. Here we provide a re-description of the type species *Hoplodoris desmoparypha* as well as descriptions of four undescribed species of *Asteronotus* and *Hoplodoris*. Bayesian inference and maximum likelihood analyses of two mitochondrial and two nuclear genes were used to evaluate the phylogenetic positions of the new species and clarify the relationships between *Asteronotus* and *Hoplodoris* to the rest of the Discodorididae. Based on our results, *Hoplodoris* is removed from synonymy with *Asteronotus*. Descriptions for ***Asteronotus markaensis* sp. nov.**, and ***Asteronotus namuro* sp. nov.** from the Red Sea, as well as ***Hoplodoris balbon* sp. nov.** and ***Hoplodoris rosans* sp. nov.** from the western Pacific are provided.

Key words: Mollusca, western Pacific, Red Sea, sea slug, biodiversity

Introduction

Nudibranch families and genera within the Doridina have been revised repeatedly over the years to better reflect hypothesized phylogenetic relationships and the corresponding revision of dorid taxonomy (Thollesson 2000; Wägele & Willan 2000; Valdés 2002; Hallas *et al.* 2017). The family Discodorididae, originally described by Bergh (1891), was composed of ten genera, which included the genus *Hoplodoris* Bergh, 1880; but would later expand to almost thirty genera including the genus *Asteronotus* Ehrenberg, 1831. Prior to uniting several genera into a single family, Odhner in Franc (1968) suggested a massive revision of numerous nudibranch families which resulted in *Hoplodoris* being re-assigned to Platydorididae, while *Asteronotus* and others were re-assigned to the family Asteronotidae. Valdés (2002) completed a morphology-based phylogenetic revision of cryptobranch dorids and found that several families including Platydorididae, Asteronotidae, Kentrodorididae, and Halgerdidae should be synonymized under Discodorididae as they shared several distinct morphological characteristics considered to be synapomorphies.

The genus *Hoplodoris* was described based on the type species *Hoplodoris desmoparypha* Bergh, 1880, which is characterized by a body with long branched tubercles, hook-shaped radular teeth, the presence of jaw rodlets, a large prostate, an armed penis with hooks, and an accessory gland with an accessory spine (Bergh 1880). The external morphology and coloration of living animals for *H. desmoparypha* is undescribed by Bergh (1880), whose description is based on preserved alcohol specimens, and the type material from Palau is presumed lost (Valdés 2002; Fahey & Gosliner 2003). However, the collection of additional specimens over time, including from the type locality of Palau, has improved the overall description for *Hoplodoris* (Thompson 1975; Miller 1991; Gosliner & Behrens 1998; Valdés 2002).

Homoiodoris novaezelandiae Bergh, 1904 was thought to be similar to *Archidoris* Bergh, 1878; however, the

Accepted by V. Padula: 5 Aug. 2020; published: 1 Dec. 2020

morphology more closely resembled that of *Hoplodoris* i.e. body with large tubercles; simple hamate radular teeth; and a large prostate. Therefore, *Homoiodoris novaezelandiae* was re-assigned into the genus *Hoplodoris* (Valdés 2002; Burn 2006). Several species that were previously assigned to the genus *Carminodoris* Bergh, 1889 were moved to the genus *Hoplodoris* after Fahey & Gosliner (2003) concluded that *Carminodoris* was a junior synonym of *Hoplodoris* based on the examination of newly collected specimens (including type species) from type localities in comparison to museum specimens. Their morphological and phylogenetic analyses resulted in several conspecific synonyms including: *H. desmoparypha*, *Carminodoris grandiflora* Pease, 1860, and *Carminodoris mauritiana* Bergh, 1891 with *Carminodoris grandiflora* having priority; *Homoiodoris novaezelandiae* with *Hoplodoris nodulosa* (Angas, 1864); and Hawaiian *Carminodoris nodulosa* Kay & Young, 1969 with *Carminodoris bifurcata* Baba, 1993. Further morphological study into the complex systematics of the Discodorididae lead to the re-allocation of the previously moved species back to *Carminodoris* after Dayrat (2010) synonymized the type species *H. desmoparypha,* as well as *Platydoris papillata* Eliot, 1904 and *Otinodoris winckworthi* White, 1948, with *Asteronotus raripilosa* (Abraham, 1877; formerly *Doris raripilosa*). Dayrat's synonymy of *H. desmoparypha* was based on morphological comparisons of numerous specimens including the type specimen of *D. raripilosa* and an extensive literature review; however, Dayrat (2010) may have misinterpreted the drastic intraspecific variation with *D. raripilosa* as a single species.

The genus *Asteronotus* Ehrenberg, 1831 is characterized by having a rigid, gelatinous body with large tubercles; no caryophyllidia; generally smooth hook-shaped radular teeth; a lobate branchial sheath; an unarmed penis with a large prostate; and an accessory gland with an accessory spine (Ehrenberg 1831; Valdés & Gosliner 2001). Species of *Asteronotus* can be variable in color as seen in *Asteronotus cespitosus* (van Hasselt, 1824), while others, such as *Asteronotus mimeticus* Gosliner & Valdés, 2002 and *Asteronotus spongicolus* Gosliner & Valdés, 2002 exhibit cryptic coloration, which may closely resemble the various sponge species on which they prey (Gosliner & Behrens 1990; Gosliner & Valdés 2002). The differences between *Asteronotus* species are usually seen in the radular teeth i.e. the shape of the outermost tooth and the presence of denticles, and the reproductive system, i.e. the size of the bursa copulatrix, the shape of the accessory gland, and the degree of curvature in the accessory spine.

Currently, the MolluscaBase (2020) lists five *Asteronotus* species: *A. cespitosus*; *Asteronotus hepaticus* (Abraham, 1877); *Asteronotus mabilla* (Abraham, 1877); *A. mimeticus*; and *A. spongicolus*; however, it should be noted that *A. mabilla* was synonymized with *A. cespitosus* by Bergh (1905) and again in Rao *et al.* (1974) reducing the number of recognized *Asteronotus* to four. Additionally, several other species including *Asteronotus brassica* (Allan, 1932); *Asteronotus fuscus* O'Donoghue, 1924; and *Asteronotus hemprichi* Ehrenberg, 1831 were also synonymized with *A. cespitosus* after a morphological review by Marcus & Marcus (1970). *Asteronotus raripilosa* (originally described as *Doris raripilosa* and currently accepted as *Otinodoris raripilosa*) remains a source of taxonomic confusion due to naming disparities between publications. Therefore, *Asteronotus raripilosa* will be referred to as *Doris raripilosa* for the purpose of this study.

Two genera have also been assessed as possible synonyms of *Asteronotus*. The genus *Peronodoris* Bergh, 1904, described based on *Peronodoris cancellata* Bergh, 1904, has been suggested to be synonymous of *Asteronotus* due to similarities in the radular teeth and the presence of an accessory spine; however, the original description is incomplete and the type material for *P. cancellata* lost, so this synonymy is still uncertain (Valdés & Gosliner 2001). The genus *Tumbia* Burn, 1962 was described as a subgenus of *Asteronotus*; however, the type material of *Tumbia trenberthi* Burn, 1962 lacks an accessory gland and the innermost and outermost radular teeth are denticulate. Therefore, Valdés & Gosliner (2001) did not consider *Tumbia* to be a synonym of *Asteronotus*, and its systematic position remains unknown. Since *Hoplodoris* is widely disputed as a recognized genus within Discodorididae and some species of *Asteronotus* have cryptic coloration, the goal of this study is to provide the first molecular phylogeny of the genus *Asteronotus* and reexamine the validity of the genus *Hoplodoris*. Here we provide a redescription of the type species, *H. desmoparypha*, and describe four new species: two species of *Asteronotus* from the Red Sea and two species of *Hoplodoris* from the western Pacific.

Material and methods

Taxon sampling. The majority of specimens used for sequencing in this study were collected primarily for molecular work and were originally preserved in 95% ethanol. Additional specimens were studied from the California

Academy of Sciences—Invertebrate Zoology wet collection and were either preserved in 70–90% ethanol or the original preservative was unknown, but successful sequencing was achieved. Specimens representing three of the four new species and all recognized species of *Asteronotus* were sequenced for this study. The holotype of *Hoplodoris balbon* **sp. nov**. was not sequenced due to DNA degradation from prior fixation using formalin. A total of 46 specimens, 31 newly sequenced and 15 with two or more genes already published and available on GenBank, were used in the phylogenetic analyses. One hundred and thirty new sequences from 41 specimens were deposited on GenBank with the following accession numbers: 16S (MN722431–MN722455, MT452884–MT452889); 28S (MN728185–MN72813, MT452656–MT452661); COI (MN720283–MN720308, MT454620–MT454623); and H3 (MN72039–MN720338, MT454624–MT454629). Sampled specimens, voucher numbers, GenBank accession numbers, and specimen localities are listed in (Table 1). Goniodorididae, Dorididae, and several members of Discodorididae were used for outgroup comparisons based on molecular phylogenetic analysis by Hallas *et al.* (2017). Voucher specimens and holotypes are deposited in the collections at the California Academy of Sciences (CASIZ) and the National Museum of Philippines (NMP).

DNA extraction, amplification and sequencing. The Qiagen DNeasy Blood and Tissue Kit (Qiagen, Valencia, CA, USA) spin column extraction method was used to extract genomic DNA from a small sample of tissue from each specimen's foot or mantle. Final DNA extractions were suspended in 50–250 µL AE buffer dependent on the size of the tissue sample and the concentration of DNA measured with a Nanodrop 2000C Spectrophotometry (ThermoFisher Scientific, Waltham, MA, USA). Double-stranded products from two mitochondrial genes (cytochrome oxidase I [COI] and 16S) and two nuclear genes (histone 3 [H3] and 28S) were amplified through polymerase chain reaction (PCR) using gene-specific primers (Suppl. Tables 1–2). These four genes were chosen based upon previous sequencing success for members of Discodorididae including *Asteronotus*; *Carminodoris* Bergh, 1889; *Diaulula* Bergh, 1878; *Discodoris* Bergh, 1877a; *Halgerda* Bergh, 1880b; *Rostanga* Bergh, 1879; *Sclerodoris* Eliot, 1904; and *Thordisa* Bergh, 1877 (Fahey 2003; Giribet *et al.* 2006; Göbbeler & Klussmann-Kolb 2010; Lindsay *et al.* 2016; Hallas *et al.* 2017; Tibiriçá *et al.* 2019). Each PCR reaction was carried out in a 25 µL volume containing: 2.5 µL of 10× PCR buffer, 0.5 µL dNTPs (10mM stock), 0.5 µL of each primer (10mM stock), 0.25 µL DreamTaq™ Hot Start DNA Polymerase (5U/µL, Thermo Fisher), 5 µL betaine, 2 µL bovine serum albumin (BSA), 2–4 µL of template DNA, and then filled to volume with Millipore-H_2O. An addition of 1 µL dimethyl sulfoxide was added to the 28S PCR amplification for secondary structure and nucleotide repeats. The PCR gene-specific protocols were run on a BioRad MyCycler Thermocycler (Bio-Rad Laboratories) at the California Academy of Sciences Center for Comparative Genomics (Suppl. Table 2). Amplified DNA was examined using gel electrophoresis on a 1% agarose gel stained with ethidium bromide. Successful single-band products were cleaned using an ExoSAP-IT protocol (USB Scientific). Samples with bold bands were cleaned using 2 µL of ExoSAP-IT with 5 µL of PCR product, while weaker bands were cleaned with 1 µL of ExoSAP-IT to 7 µL of PCR product. In PCR reactions that yielded double banding, the correct gene fragment was cleaned using gel excision. The clean PCR products were then fluorescently labeled with dye-terminators (Big Dye 3.1, Applied Biosystems) during cycle sequencing following SteP protocol (Platt *et al*. 2007). Each reaction contained: 1.5 µL of 5× reaction buffer, 0.3 µL of primer (10 mM stock), 0.75 µL of Big Dye, 4.45–5.45 µL of Millipore-H_2O, and 2–3 µL of cleaned PCR product. The newly labeled single-stranded DNA was precipitated using 2.5 µL of EDTA followed by washing and centrifugation of 100% ethanol (30 µL) and 70% ethanol (60 µL), before placement in a 60°C incubator to evaporate any residual ethanol. HiDi formamide (10 µL, Applied BioSystems) was added to each DNA pellet, which was then denatured in a BioRad MyCycler Thermocycler (Bio-Rad Laboratories) at 95°C for 2 min and then immediately cooled on ice for 5 min. Both directions of the denatured, fluorescently labeled DNA fragments were sequenced on an ABI3130 Genetic Analyzer in the Center for Comparative Genomics at the California Academy of Sciences.

Sequence alignment and analyses. Both strands of each gene fragment sequenced were assembled, trimmed to remove primers, and edited using Geneious v11.1.5 (Kearse *et al*. 2012) and Mesquite v3.51 (Maddison & Maddison 2018). Sequences were aligned with MAFFT (Katoh *et al.* 2009) using algorithm E-INS-I while additional editing for the 16S and 28S alignments was done by hand. Gene saturation and the number of parsimonious informative characters were determined for each gene using PAUP v4.0a167 (Swofford 2003). Saturation was checked by plotting uncorrected *p*-distances for transitions + transversions against the uncorrected *p*-distances for all substitutions for each codon position in COI and H3. Saturation in 16S and 28S was checked by plotting the uncorrected *p*-distances for transitions + transversions against the total number of character differences. Evolutionary relationships for all genetic markers were analyzed independently and then concatenated using Bayesian

TABLE 1. Data of specimens successfully sequenced and dissected. Species names represent current proposed taxonomy. Dashes indicate missing sequences.

Specimen	Voucher	Accession Numbers				Locality
		16S	28S	COI	H3	
Goniodoridídae						
Ancula gibbosa	CASIZ 182028	KP340291	KP340356	KP340388	KP340413	Cape Elizabeth, Cumberland County, Maine, USA
Doridídae						
Aphelodoris sp. 1	CASIZ 176920	MF958293	MF958379	MF958424	–	Oudekraal, Cape Province, South Africa
Discodoridídae						
Atagema notacristata	CASIZ 167980	KP871681	MT452661	KP871634	KP871657	Isla Uva, Golfo de Chiriqui, Panama
Carminodoris flammea	CASIZ 177628	MN722433	MN728190	MN720285	MN720311	Calumpan Peninsula, Batangas Province, Luzon Island, Philippines
Carminodoris nodulosa	EED-Phy-959	FJ917428	FJ917469	FJ917486	–	New South Wales, Australia
Diaulula sandiegensis	CASIZ 181321	MN722435	MN728193	MN720287	MN720317	Scott Creek, Santa Cruz County, California, USA
Discodoris boholiensis	CASIZ 204802	MN722451	MN728210	MN720304	MN720335	Puerto Galera, Oriental Mindoro Province, Philippines
Discodoris cebuensis	CASIZ 190761	MN722440	MN728200	MN720293	MN720322	Rasch Passage, Madang Province, Papua New Guinea
Geitodoris heathi	CASIZ 181314	KP871690	MN728192	KP871642	KP871666	Carmel Point, Monterey County, California, USA
Halgderda carlsoni	CASIZ 177575	KP871691	MN728189	KP871643	KP871667	Red Palm, Maricaban Island, Batangas Province, Philippines
Halgerda dalanghita	CASIZ 181264	MF958289	MF958376	MF958420	MN720316	Devil's Point, Maricaban Island, Batangas Province, Philippines
Peltodoris nobilis	CASIZ 182223	HM162593	MN728194	HM162684	HM162499	Pillar Point, San Mateo County, California, USA
Platydoris sanguinea	CASIZ 177762	MF958285	MF958372	MF958416	MN720312	Devil's Point, Maricaban Island, Batangas Province, Philippines
Rostanga calumus	EED-Phy-935	FJ917427	FJ917468	FJ917485	–	New South Wales, Australia
Sclerodoris sp.	CASIZ 182866	MN722437	MN728196	MN720289	MN720319	Balayan Bay, Batangas Province, Luzon Island, Philippines
Sclerodoris sp.	CASIZ 191525	MN722444	MN728204	MN720297	MN720328	Cement Mixer Reef, Madang Province, Papua New Guinea
Sclerodoris tuberculata	CASIZ 190788	MF958286	MF958373	MF958417	MN720323	Cement Mixer Reef, Madang Province, Papua New Guinea
Taringa sp.	CASIZ 172039	MN722432	MN728186	MN720284	MN720310	Tortuga, Isla Santa Cruz, Galapagos Island, Ecuador
Taringa telopia	CASIZ 182933	KP871700	MN728198	MN720291	KP871675	Bocas Del Toro, Panama
Thordisa albomacula Clade A	CASIZ 181136	MN722434	MN728191	MN720286	MN720314	Bigej-Meck, Kwajalein Atoll, Marshall Islands, Pacific Ocean
Thordisa albomacula Clade A	CASIZ 220322	MT452884	–	MT454620	MT454624	Maalaea Bay, Maui, Hawaii, USA
Thordisa albomacula Clade B	CASIZ 177688	MT452886	MT452657	–	MT454626	Maricaban Island, Batangas Province, Luzon Island, Philippines
Thordisa albomacula Clade B	CASIZ 181345	MT452885	MT452656	MT454621	MT454625	Bigej-Meck, Kwajalein Atoll, Marshall Islands, Pacific Ocean

.....continued on the next page

TABLE 1. (Continued)

Specimen	Voucher	Accession Numbers				Locality
		16S	28S	COI	H3	
Thordisa albomacula Clade B	CASIZ 190821	MT452887	MT452658	–	MT454627	Tabad Island, Madang Province, Papua New Guinea
Thordisa albomacula Clade C	CASIZ 179586	MT452889	MT452660	MT454623	MT454629	Bigej-Meck, Kwajalein Atoll, Marshall Islands, Pacific Ocean
Thordisa albomacula Clade C	CASIZ 179590	MF958287	MF958374	MF958418	MN720313	Bigej-Meck, Kwajalein Atoll, Marshall Islands, Pacific Ocean
Thordisa albomacula Clade C	CASIZ 182834	MT452888	MT452659	MT454622	MT454628	Balayan Bay, Batangas Province, Luzon Island, Philippines
Thordisa bimaculata	CASIZ 184516	MN722439	MN728199	MN720292	MN720321	Naples, Santa Barbara County, California
Asteronotus cespitosus	CASIZ 177226	KP871680	MN728188	KP871633	KP871656	Balayan Bay, Batangas Province, Luzon Island, Philippines
Asteronotus cespitosus	CASIZ 191321	MN722443	MN728203	MN720296	MN720327	Madang Province, Papua New Guinea
Asteronotus cespitosus	CASIZ 191163	MN722441	MN728201	MN720294	MN720325	Kranket Island, Madang Province, Papua New Guinea
Asteronotus cespitosus	CASIZ 191096	MF958288	MF958375	MF958419	MN720324	Kranket Island, Madang Province, Papua New Guinea
Asteronotus hepaticus	CASIZ 191310	MN722442	MN728202	MN720295	MN720326	Madang Province, Papua New Guinea
***Asteronotus markaensis* sp. nov.**	CASIZ 192316A	MN722446	MN728206	MN720299	MN720330	Marka Island, Red Sea, Saudi Arabia
Asteronotus mimeticus	CASIZ 208221	MN722452	MN728211	MN720305	MN720336	Verde Island, Batangas Province, Luzon Island, Philippines
***Asteronotus namuro* sp. nov.**	CASIZ 192297	MN722445	MN728205	MN720298	MN720329	Tigerhead Island, Red Sea, Saudi Arabia
Asteronotus spongicolus	CASIZ 192317A	MN722447	MN728207	MN720300	MN720331	Kaust Beach, Thuwal, Makkah Province, Red Sea, Saudi Arabia
Asteronotus spongicolus	CASIZ 194597	MN722448	MN728208	MN720301	MN720332	Sepok, Maricaban Island, Batangas Island, Philippines
Asteronotus spongicolus	CASIZ 200581A	MN722449	–	MN720302	MN720333	Lubang Island, Occidental Mindoro, Philippines
Asteronotus spongicolus	CASIZ 200662	MN722450	MN728209	MN720303	MN720334	Deep Wall, Lubang Island, Occidental Mindoro, Philippines
Asteronotus spongicolus	CASIZ 227580A	MN722453	MN728212	MN720306	MN720337	Barracuda Point, East Coast, Zanzibar, Tanzania
Asteronotus spongicolus	CASIZ 227581	MN722454	MN728213	MN720307	MN720338	Barracuda Point, East Coast, Zanzibar, Tanzania
***Hoplodoris balbon* sp. nov.**	CASIZ 171406	–	–	–	–	Panglao, Bohol Island, Philippines
Hoplodoris desmoparypha	CASIZ 309550	MN722455	–	MN720308	–	Ngermutidech, Koror Island, Palau
Hoplodoris desmoparypha	CASIZ 70066	MN722431	MN728185	MN720283	MN720309	Seragaki Beach, Maeki-zaki, Okinawa, Ryukyu, Japan
***Hoplodoris rosans* sp. nov.**	CASIZ 182837	MN722436	MN728195	MN720288	MN720318	Calumpan Peninsula, Batangas Province, Luzon Island, Philippines
***Hoplodoris rosans* sp. nov.**	CASIZ 182921	MN722438	MN728197	MN720290	MN720320	Calumpan Peninsula, Batangas Province, Luzon Island, Philippines

Inference (BI) and Maximum Likelihood (ML). Best-fit evolution model partition definitions for the BI and ML analyses were determined using PartitionFinder2 (Lanfear *et al*. 2016) on XSEDE via the online CIPRES Science Gateway (Miller *et al*. 2010). The concatenated dataset was partitioned by gene and codon. Bayesian inference was performed in MrBayes v3.2.7a (Ronquist & Huelsenbeck 2003). The dataset was run for 5×10^7 generations, with Markov chains sampled every 1000 generations, and the standard 25% burn-in calculated. Convergence of the two chains was checked using TRACER v1.7.1 (Drummond & Rambaut 2007) and a 50% majority rule consensus tree of calculated posterior probabilities (pp) was created from the remaining tree estimates. Tree branches were considered strongly supported if posterior probability values were ≥ 0.95, while values ≤ 0.94 were considered to have low support (Alfaro *et al.* 2003). Randomized accelerated maximum likelihood (RAxML) v8.2.12 (Stamatakis 2014) was used to estimate non-parametric bootstrap values with the evolution model GTR+GAMMA+I and was set for 5×10^4 fast bootstrap runs. Branches with bootstrap values of ≥ 70 were considered strongly supported, while those with values ≤ 70 were considered weakly supported (Alfaro *et al.* 2003). All alignments and trees are deposited in TreeBASE (http://purl.org/phylo/treebase/phylows/study/TB2:S26800). Species delimitation and ingroup diversity were determined using Automatic Barcode Gap Discovery (ABGD) analysis outlined by Puillandre *et al.* (2012) and Bayesian Poisson tree process (bPTP) by Zhang *et al.* (2013). The mitochondrial COI gene was chosen for ABGD species delimitation based on previous delimitation success within Discodorididae in the species complex *Diaulula sandiegensis* (J.G. Cooper, 1863) (Lindsay *et al.* 2016) and the genus *Halgerda* (Tibiriçá *et al.* 2019).

Species delimitation analyses. The ABGD method is designed to detect barcode gaps or breaks between intraspecific and interspecific variation via genetic pairwise distances (uncorrected *p*-distances). An ingroup COI alignment created in Mesquite v3.51 was uploaded to the ABGD Web-based interface (https://bioinfo.mnhn.fr/abi/public/abgd/abgdweb.html). Since ABGD analysis requires the integration of previous analysis conducted by others to decide on settings (Kekkonen *et al.* 2015), we tested Jukes-Cantor (JC69), Kimura (K80), and Simple Distances as well as different gap widths (Fig. S1) to evaluate which settings were congruent with our own phylogenetic analysis. The following parameters were applied: Jukes-Cantor (JC69) P.min = 0.001, P.max = 0.1, Steps = 10, NB = 20, but with a relative gap width × = 1.5. Bayesian PTP models the number of substitutions between branchings i.e. the branch lengths of a previously inputted phylogenetic tree, using Bayesian MCMC methods to identify groups descended from a single ancestor (Zhang *et al.* 2013). This test was performed on the four gene concatenated dataset (16S + 28S + COI + H3) resulting from the BI analysis using the bPTP server (https://species.h-its.org/). The following parameters were applied: 100,000 generations, 100 thinning, 0.1 burn-in, and 123 seeds. Convergence was checked using the ML convergence plot generated by the bPTP server.

Morphological analysis. Specimens were dissected along the center of the foot using a Nikon SMZ-U dissection microscope to remove the buccal mass and reproductive system. Skin samples were taken from the dorsal side of the mantle to closely examine tubercle/papillae size and structure and mounted on glass coverslips for examination by scanning electron microscope (SEM). The buccal mass was dissolved in 10% sodium hydroxide (NaOH) for 12–24 h. The jaws and radula were then rinsed with deionized water and mounted on glass coverslips for SEM imaging. The arrangement of the reproductive organs was hand-drawn using a camera lucida drawing attachment on the Nikon SMZ-U dissection microscope. The reproductive accessory spines and penial spines were dissected from the accessory gland and penis, respectively, and mounted on glass coverslips for SEM imaging. Due to small size, accessory spines from the newly described *Asteronotus* specimens were soaked in 75% ethanol mixed with acid fuchsin stain; and then rinsed sequentially in 95% ethanol, 100% ethanol, and xylene before being permanently mounted on glass slides for examination. SEM samples were coated with gold/palladium using a Cressington 108 Auto vacuum sputter coater. Micrographs were taken of the jaws, radula, teeth, penial and accessory spines, and skin using a Hitachi SU3500 scanning electron microscope. The permanently mounted *Asteronotus* accessory spines were imaged using a Leica DM750 transmitted light microscope and processed using Leica Application Suite (v4.12). Specimens and dissected structures were deposited at the California Academy of Sciences Department of Invertebrate Zoology (CASIZ) collection and the National Museum of Philippines (NMP).

Results

Phylogenetic and species delimitation analyses. The final four-gene concatenated dataset was 2,270 bp in length including gaps, while the edited and aligned lengths for 16S, 28S, COI, and H3 were 453, 829, 658, and 330 bp,

respectively. In some specimens not all four genes were successfully sequenced, and occasionally only partial sequences were obtained (Table 1). In the single gene alignments, COI had 247 parsimonious informative characters, while 28S had 130, 16S had 115, and H3 had 85 informative characters. The BI and ML analyses resulted in similar topologies for the concatenated dataset (Fig. 1) and the individual gene trees (Figs. S2–S5). Overall, the individual gene trees (Figs. S2–5) yielded moderately poor resolution in comparison with the concatenated tree. The mitochondrial single-gene 16S (Fig. S2) was mostly unresolved; however, it did recover two strongly supported clades of *Asteronotus*, but failed to recover both species of *Hoplodoris* together. The poor resolution within the 16S tree may be explained by a high number of recently diverged species combined with low genetic divergence within the 16S dataset (Xia *et al.* 2012). The nuclear single-gene 28S (Fig. S3) and the mitochondrial single-gene COI (Fig. S4) provided the most resolution within the single-gene trees. Within the 28S tree, there are two strongly supported *Asteronotus* clades and a strongly supported clade of *Hoplodoris*; however, the relationship between the two *Asteronotus* clades is unresolved and a specimen of *H. rosans* (CASIZ 182837) grouped together with *H. desmoparypha* (CASIZ 70066), rather than the other *H. rosans* specimen. The COI tree was unable to resolve the relationships between the two major clades of *Asteronotus* and the two species of *Hoplodoris*; however, species delimitation analyses successfully detected eight distinct species between *Asteronotus* and *Hoplodoris*. Missing data from both partial sequences and a few specimens may explain the unresolved relationships within our COI and highly conserved 28S datasets (Moore & Gosliner 2011). The nuclear single-gene H3 (Fig. S5) successfully recovered all specimens of *Asteronotus* in one clade; however, one specimen of *A. spongicolus* (CASIZ 200581A) grouped together with *A. hepaticus* rather than the other five specimens of *A. spongicolus*. The slow evolution of the nuclear H3 gene may explain why the H3 tree was unable to separate the polytomy between *H. rosans* and *H. desmoparypha* (e.g. Malaquias *et al.* 2009; Ortigosa *et al.* 2014; Pola *et al.* 2014; Tibiriçá *et al.* 2019).

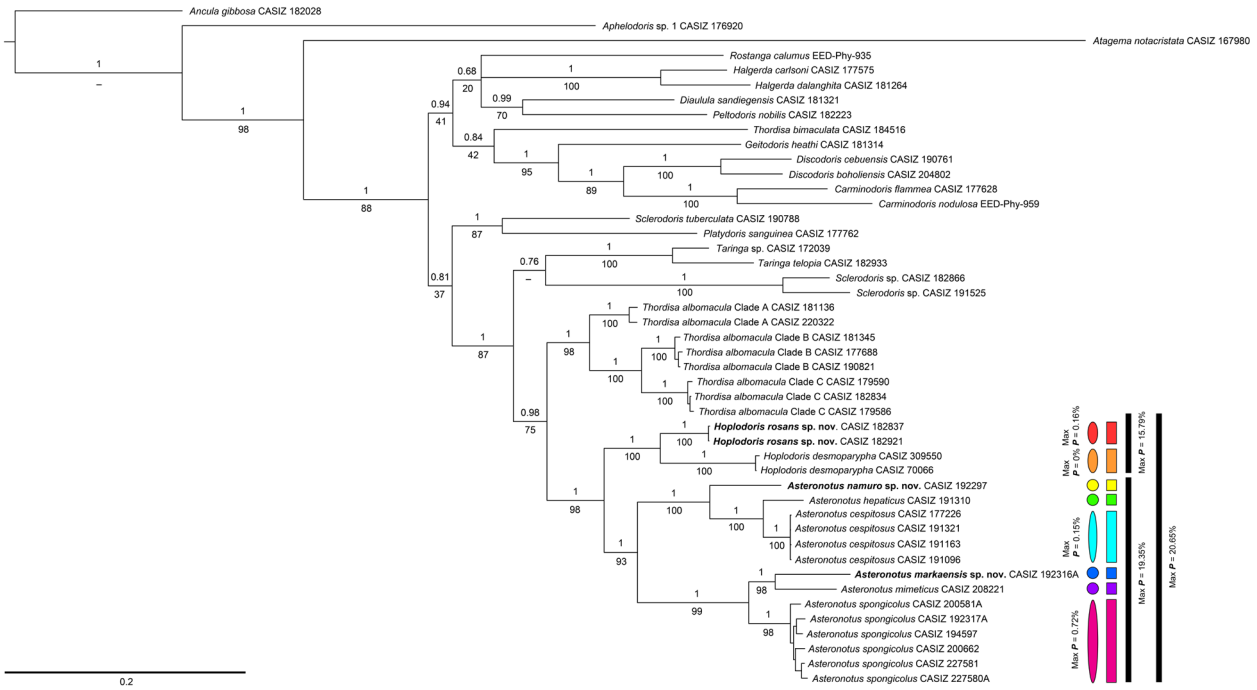

FIGURE 1. Phylogenetic tree of the *Asteronotus* Ehrenberg, 1831 and *Hoplodoris* Bergh, 1880 estimated from the four gene (16S+28S+COI+H3) concatenated data set based on Bayesian Inference (BI) and Maximum Likelihood (ML) analyses. Numbers above branches refer to BI posterior probabilities (pp), while numbers below branches refer to ML non-parametric bootstrapping values (bs). Relationships not recovered during ML analysis are indicated by dashes. To the right are the results of the ABGD analysis (oval), bPTP analysis (square) and maximum pairwise distances.

In all trees, the BI analysis usually showed better nodal support then the ML analysis; however, both analyses support the monophyly of *Hoplodoris* (pp=1; bs=100) and *Asteronotus* (pp=1; bs=93). In this study, *Hoplodoris*, rather than *Thordisa*, is strongly supported as the sister taxon of *Asteronotus* (pp=1; bs=98). Both *Asteronotus* and *Hoplodoris* are strongly related (pp=0.98; bs=75) to a clade of *Thordisa albomacula* Chan & Gosliner, 2007. *Asteronotus* is split into two well-supported clades. The first is composed of *Asteronotus namuro* Donohoo & Gosliner

sp. nov., *A. hepaticus*, and *A. cespitosus* (pp=1; bs=100). The second contains cryptic species including *Asteronotus markaensis* Donohoo & Gosliner **sp. nov.**, *A. mimeticus*, and *A. spongicolus* (pp=1; bs=99). Within *Hoplodoris*, the type species, *H. desmoparypha* and the newly described species *Hoplodoris rosans* Donohoo & Gosliner **sp. nov.** are well-supported (pp=1; bs=100 and pp=1; bs=100, respectively).

ABGD analysis of the genetic pairwise distances in the aligned COI dataset and the bPTP analysis of the concatenated dataset resulted in two distinct species of *Hoplodoris* and six distinct species of *Asteronotus*. The maximum genetic distance of all sequenced *Asteronotus* was 19.55%, while the maximum distance was 16.07% in *Hoplodoris*. The interspecific distance between *Asteronotus* and *Hoplodoris* was 16.47−21.01%, while intraspecific variation was 0.15−0.34% within *A. cespitosus*, 0.72−2.44% within *A. spongicolus*, and 0.16% in *H. desmoparypha* (Table 2). No intraspecific variation was found in the two specimens of *H. rosans* studied here.

TABLE 2. Pairwise uncorrected *p*-distances (%) for COI between *Asteronotus* and *Hoplodoris* spp.

		1	2	3	4
1	*Asteronotus cespitosus*	0.15–0.34			
2	*Asteronotus hepaticus*	9.28–9.55	–		
3	*Asteronotus spongicolus*	16.36–17.49	16.79–17.94	0.72–2.44	
4	***Asteronotus markaensis* sp. nov.**	15.71–16.10	16.10	13.01–13.67	–
5	*Asteronotus mimeticus*	19.35–19.55	17.76	12.82–13.67	12.92
6	***Asteronotus namuro* sp. nov.**	14.55–14.99	16.60	17.25–18.56	15.51
7	*Hoplodoris desmoparypha*	16.47–16.87	16.87	19.78–21.01	17.90–18.10
8	***Hoplodoris rosans* sp. nov.**	16.65–17.37	18.07–18.14	17.10–18.78	17.83–17.90

TABLE 2. (Continued)

		5	6	7	8
1	*Asteronotus cespitosus*				
2	*Asteronotus hepaticus*				
3	*Asteronotus spongicolus*				
4	***Asteronotus markaensis* sp. nov.**				
5	*Asteronotus mimeticus*	–			
6	***Asteronotus namuro* sp. nov.**	19.15	–		
7	*Hoplodoris desmoparypha*	20.61–20.82	16.47	0.16	
8	***Hoplodoris rosans* sp. nov.**	19.35–19.42	16.91–16.98	15.99–16.07	–

Systematics

Order Nudibranchia Cuvier, 1817

Family Discodorididae Bergh, 1891

Genus *Asteronotus* Ehrenberg, 1831

Type Species: *Asteronotus hemprichi* Ehrenberg, 1831 = *Asteronotus cespitosus* (van Hasselt, 1824) by monotypy

Diagnosis. Rigid, gelatinous body covered with large, simple, rounded tubercles. Lobate branchial sheath. Labial cuticle unarmed. Reproductive system composed of a granular prostate with two differentiated sections. Vagina unarmed. Penis unarmed. Granular accessory gland armed with an accessory spine (Valdés 2001). Broad foot, anteriorly notched. Head with two conical oral tentacles. Radula composed of simple, hamate teeth with some denticulation (present study).

***Asteronotus markaensis* sp. nov.**
(Figs. 2A, 3, 4A, 5A)
urn:lsid:zoobank.org:act:1645B16B-8D63-43A6-B108-CA4DC468BB64

Asteronotus sp.—Gosliner *et al*. 2015: page 182, top right photograph. Gosliner *et al.* 2018: page 102, bottom left photograph.

Type material. **Holotype**: CASIZ 192316A, one specimen, dissected, foot subsampled for molecular analyses, Marka Island, 18.22668° N 41.31740° E, Red Sea, Saudi Arabia, 7.9m depth, 06 March 2013, T.M. Gosliner. **Paratypes**: CASIZ 192316B, one specimen. Marka Island, 18.22668° N 41.31740° E, Red Sea, Saudi Arabia, 7.9m depth, 06 March 2013, T.M. Gosliner.

Type locality. Marka Island, Saudi Arabia, Red Sea.

External morphology. The living animals (Fig. 2A) are oval in shape, range in length between 10–20 mm, and are found under foliose sponges on reef flats between 8–9m. The body color is medium to dark grey with scattered dark flecking predominantly along the edge of the mantle. The underside of the mantle is tan with a few scattered dark flecks concentrated near the oral tentacles. Light grey tubercles are arranged in irregular groups across the mantle and may also have opaque white spotting along the tips. The gill surrounds the anus and has eight dark grey bipinnate branchial leaves with opaque white spotting along the rachises. The gill pocket contains eight distinct lobes with gentle crenulations that are similar in color to the rest of the body. The rhinophores are perfoliate with 6–10 grey lamellae. The foot is broad, anteriorly notched, and tan in color with scattered dark flecking along the dorsal side. An elongate, digitiform oral tentacle is found laterally on either side of the labial region and mouth.

Internal anatomy. *Buccal mass and radula.* The buccal mass is muscular and anteriorly connects to a thin labial cuticle which is devoid of armature or rodlets. The radula (Fig. 3A) is composed of predominantly smooth hamate teeth and the radular formula is 44 × 23.0.23 in the holotype CASIZ 192316A. The inner lateral four to five teeth (Fig. 3B) are short with a broad base and a curved cusp. Some of the inner teeth have a single triangular denticle along the outer side of the primary cusp. The middle lateral teeth (Fig. 3C) are larger and more elongate than the inner teeth with a smooth, narrow cusp. The outer lateral teeth (Fig. 3D) are also larger and elongate, but have a much shorter, rounder smooth cusp than the middle laterals.

Reproductive System. From a narrow preampullary duct, the convoluted ampulla expands before folding and narrowing into the vas deferens and a short oviduct (Fig. 4A). The vas deferens enter an irregular, wide prostate that abruptly narrows distally before elongating into a muscular, ejaculatory portion connected to the penis which enters the common genital atrium shared with the vagina. A narrow, elongate vagina enters a bursa copulatrix that is smaller than the prostate. A short duct connects near the base of the bursa to an elongate receptaculum seminis. The uterine duct also connects to the base of the receptaculum and enters the female gland mass. A sessile elongate nodular accessory gland enters the common genital atrium between the penis and the vagina. Within the base of the accessory gland is a semi-elongate strongly curved accessory spine with a wide base (Fig. 5A).

Etymology. This species is named *Asteronotus markaensis* after the type locality Jazirat Marka or Marka Island, which is found in the Saudi Arabian Red Sea.

Geographical distribution. Known only from the Saudi Arabian Red Sea.

Remarks. In our molecular phylogeny, *Asteronotus markaensis* is part of a clade of cryptic species that includes *A. spongicolus* (Fig. 2B) and *A. mimeticus* (Fig. 2C). *Asteronotus markaensis* is sister to *A. mimeticus* and closely related to *A. spongicolus*. All three are to some extent externally similar; however, our ABGD and bPTP analyses reveal that there is a strong genetic divergence of 12.92% in the COI gene between *A. markaensis* and *A. mimeticus*; as well as a minimum divergence of 13.01% between *A. markaensis* and *A. spongicolus*. These high genetic differences combined with key differences in the internal morphology support *A. markaensis* as a distinct species. Externally, *A. markaensis* is a medium to dark grey with numerous irregular groups of light grey tubercles that cover the entire body; whereas, *A. mimeticus* body coloration is grey, brown, or yellow and either entirely smooth or it may have a few groups of tubercles and elongated papillae (Gosliner & Valdés 2002, figs. 1A–D). The body coloration of *Asteronotus spongicolus* is green or brown with scattered spots a central line of light pigment along the body and is either entirely smooth or with very few tubercles (Gosliner & Valdés 2002, figs. 1E–F). Gosliner and Valdés (2002) described the variability of color and texture in the tropical *A. mimeticus* and *A. spongicolus* as a reflection of the variability in sponge prey species potentially due to their wide geographical distribution. *Asteronotus mimeticus* is found throughout the western Pacific Ocean, while *A. spongicolus* is widespread throughout both the Indian and

western Pacific oceans including the Red Sea. This type of color and prey variation may also occur in the newly described *A. markaensis* from the Red Sea; however, additional specimens are required to confirm whether this variability is present.

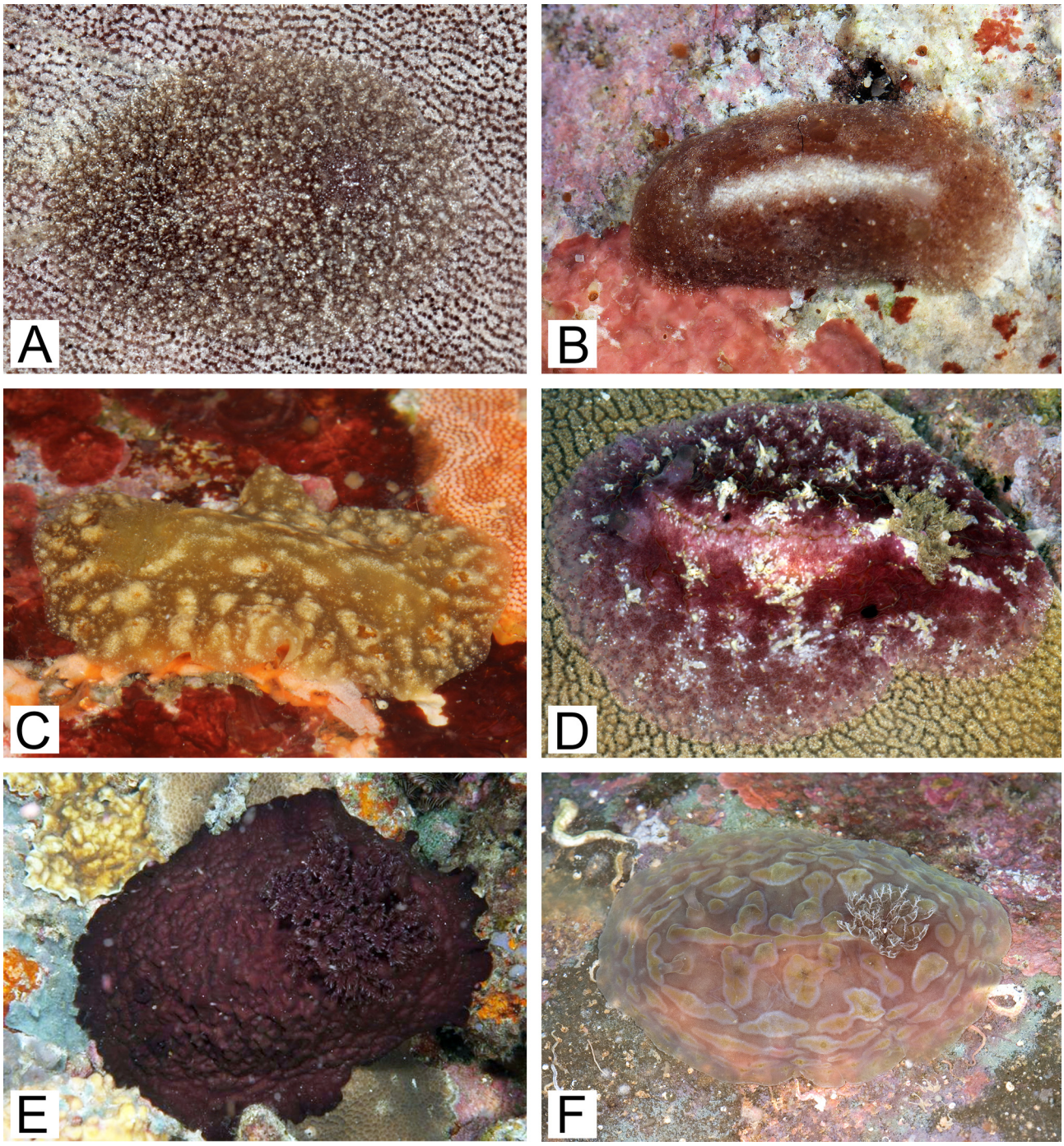

FIGURE 2. *Asteronotus*, living specimens. **A**. *Asteronotus markaensis* **sp. nov.** CASIZ 192316A, Saudi Arabian Red Sea; **B**. *Asteronotus spongicolus* CASIZ 194597, Philippines; **C**. *Asteronotus mimeticus* CASIZ 208221, Philippines; **D**. *Asteronotus namuro* **sp. nov.** CASIZ 192297, Saudi Arabian Red Sea; **E**. *Asteronotus hepaticus*, uncollected. **F**. *Asteronotus cespitosus* CASIZ 177226, Philippines. Photos (A–D, F by Terry Gosliner) and (E by Alicia Hermosillo).

The radular teeth are similar in shape between *A. markaensis*, *A. mimeticus,* and *A. spongicolus*; but the presence of denticles and the shape of the outermost tooth vary. In *A. markaensis*, some of the inner five lateral teeth have a single triangular denticle on either side of the cusp, while most of the *A. mimeticus* specimens studied in Gosliner and Valdés (2002) had no denticles; however, one specimen of *A. mimeticus* from Papua New Guinea had one to two triangular denticles on the outer edge of the cusp on the innermost 14 teeth (Gosliner & Valdés 2002,

figs. 4C–D). In contrast, the innermost teeth of *A. spongicolus* have one to two denticles along the inner cusp, followed by an additional seven teeth having one to two denticles along the outer cusp (Gosliner & Valdés 2002, figs. 7A–B). In all *A. mimeticus* specimens studied the outermost tooth is reduced to an ovoid plate (Gosliner & Valdés 2002, fig. 7D), while the outermost tooth in *A. spongicolus* is reduced to a quadrangular plate (Gosliner & Valdés 2002, figs. 3D, 4B, 4D), but in *A. markaensis* the outermost tooth is simply a reduced version of the rest of the outer lateral teeth and is narrow and elongate.

The reproductive system of *A. markaensis* has a large irregular prostate with a smaller bursa copulatrix and a smaller elongate receptaculum seminis; whereas *A. mimeticus* has a large bursa copulatrix, a smaller rounded receptaculum seminis, and a smaller prostate (Gosliner & Valdés 2002, fig. 5), while *A. spongicolus* has a large receptaculum seminis, a slightly smaller bursa copulatrix, and a small wide prostate (Gosliner & Valdés, 2002, fig. 8). Furthermore, the accessory gland in *A. markaensis* is sessile, rounded and elongate with a shorter, strongly curved accessory spine; whereas, the accessory gland in *A. spongicolus* is more irregular with a similarly curved accessory spine; however, the base is much broader and the cusp more narrow (Gosliner & Valdés 2002, fig. 6C). In contrast to *A. markaensis* and *A. spongicolus* the accessory gland in *A. mimeticus* is more regular in shape with an elongate, slightly curved accessory spine (Gosliner & Valdés 2002, figs. 6A–B).

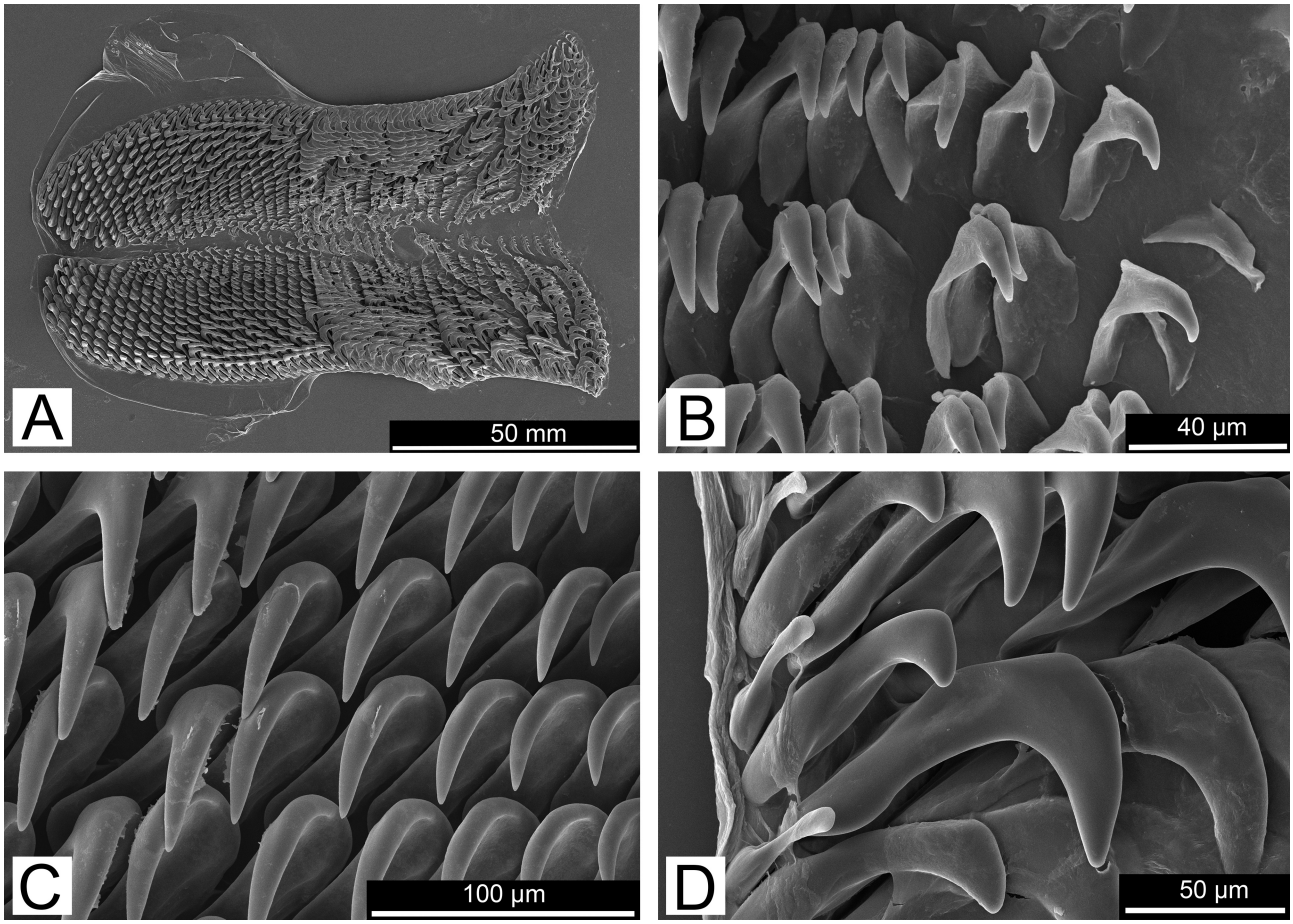

FIGURE 3. *Asteronotus markaensis* **sp. nov.** CASIZ 192316A. Radula, scanning electron micrographs. **A**. Entire radula; **B**. Central teeth; **C**. Mid-lateral teeth; **D**. Outer lateral teeth.

***Asteronotus namuro* sp. nov.**
(Figs. 2D, 4B, 5B, 6)
urn:lsid:zoobank.org:act:A7E57F60-38DA-4AD9-85DC-940DA349736F

Thordisa sp. 16—Gosliner *et al*. 2015: page 182, top left photograph.
Thordisa sp. 18—Gosliner *et al*. 2018: page 103, middle right photograph.

Type material. **Holotype**: CASIZ 192297, one specimen, dissected, foot subsampled for molecular analyses, Tigerhead Island, 16.79097° N 41.199012° E, Red Sea, Saudi Arabia, 17.4m depth, 10 March 2013, T.M. Gosliner.

Type locality. Tigerhead Island, Saudi Arabia, Red Sea.

External morphology. The living animals (Fig. 2D) are oval in shape, approximately 45–55 mm in length, and were found under coral rubble on steep sandy slopes 17m in depth. The body color is a pinkish pale red with random dark red and white flecks that increase in concentration moving away from the mantle's edge; numerous red and white tubercles that vary in size; and random dark red blotches surrounding a medially light pink crest with a central brown line. The underside of the mantle is a pinkish pale red color with random dark-red flecks across the entire mantle. The gill surrounds the anus and consists of 6 light brown tripinnate brachial leaves with light brown rachises and scattered opaque white spots. The gill pocket consists of six distinct lobes that are red in color with a large patch of white at the apex. The rhinophores are perfoliate with 15–20 dark purple lamellae. The base and middle regions of the rhinophores are purple with scattered red spots. The two rhinophoral sheaths are crenulated and purple in color with random patches of reddish pink. The foot is broad, anteriorly notched, and cream in coloration with random red flecks. An elongate, digitiform oral tentacle is found laterally on either side of the labial region and mouth.

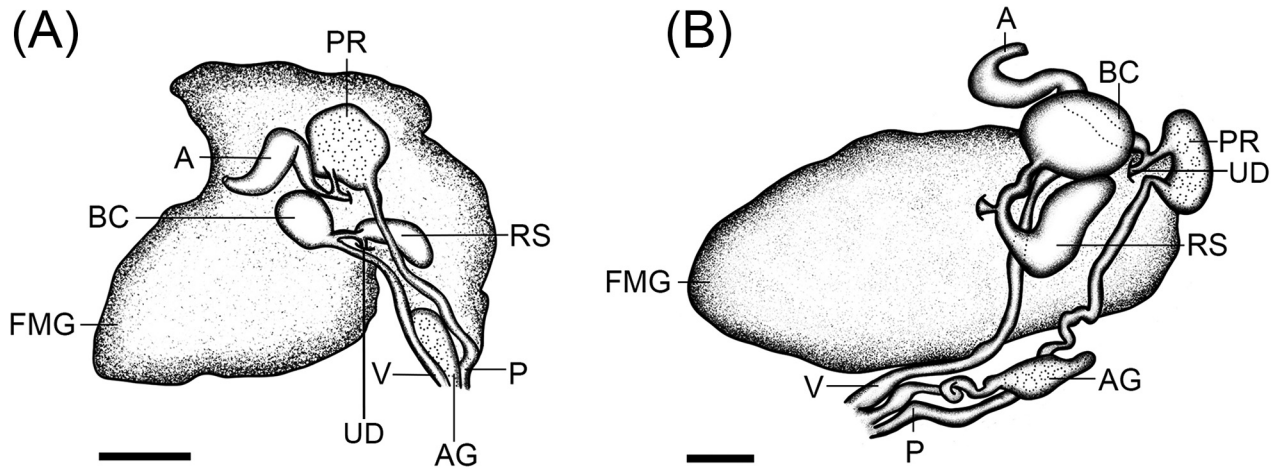

FIGURE 4. *Asteronotus*, reproductive system. **A**. *Asteronotus markaensis* **sp. nov.** CASIZ 192316A(scale bar = 1mm).**B**. *Asteronotus namuro* **sp. nov.** CASIZ 192297 (scale bar = 1mm). Abbreviations: A, ampulla; AG, accessory gland; BC, bursa copulatrix; FGM, female gland mass; P, penis; PR, prostate; RS, receptaculum seminis; UD, uterine duct; V, vagina.

Internal morphology. *Buccal mass and radula.* The buccal mass is muscular and anteriorly connects to a thin labial cuticle which is devoid of armature or rodlets. The radula (Fig. 6A) is composed of predominantly smooth hamate teeth and has the radular formula 34 × 29.0.29 in the holotype CASIZ 192297. The inner lateral teeth (Fig. 6B) are short with a broad base which abruptly curve at the cusp. The first tooth of the inner teeth has one to two triangular denticles along either the outer side of the cusp. The remainder of the inner laterals are smooth. The middle lateral teeth (Fig. 6C) are larger with a shorter, elongated narrow cusp and lack denticles. The outer lateral teeth (Fig. 6D) are also larger and slightly elongate, but have a shorter, rounder cusp than the middle laterals and also lack denticles.

Reproductive system. A thin preampullary duct widens into a thick ampulla that abruptly narrows into the vas deferens and a short oviduct (Fig. 4B). The vas deferens widens into an ovoid prostate, which quickly narrows distally into a convoluted, elongate muscular ejaculatory portion. The ejaculatory portion connects with an elongate penis which shares a common genital atrium with the accessory gland and vagina. A narrow, elongate vagina enters a rounded bursa copulatrix that is larger than the prostate. A short, thick duct connects the bursa to the irregular receptaculum seminis, while the uterine duct also connects near the base of the receptaculum and enters the female gland mass. An irregular-shaped nodular accessory gland is connected to the common genital atrium by a convoluted, looping, elongate duct. Within the base of the accessory gland is an elongate, slightly curved accessory spine with a broad base (Fig. 5B).

Etymology. This species is named *Asteronotus namuro* after "namur" the Arabic word for tiger, since the type material is found around Tigerhead Island.

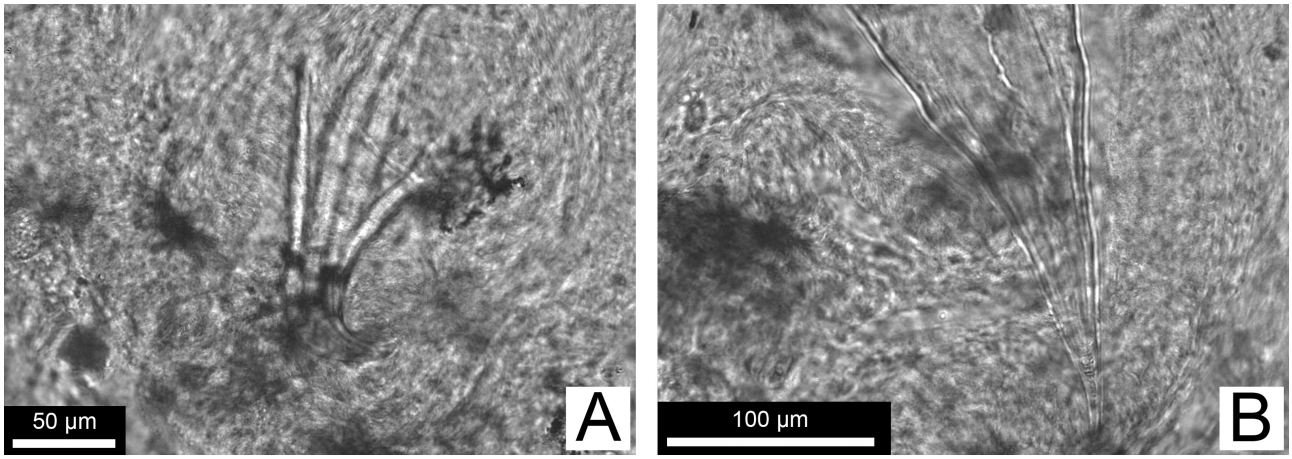

FIGURE 5. *Asteronotus*. Accessory spines, light micrographs. **A**. *Asteronotus markaensis* **sp. nov.** CASIZ 192316A; **B**. *Asteronotus namuro* **sp. nov.** CASIZ 192297.

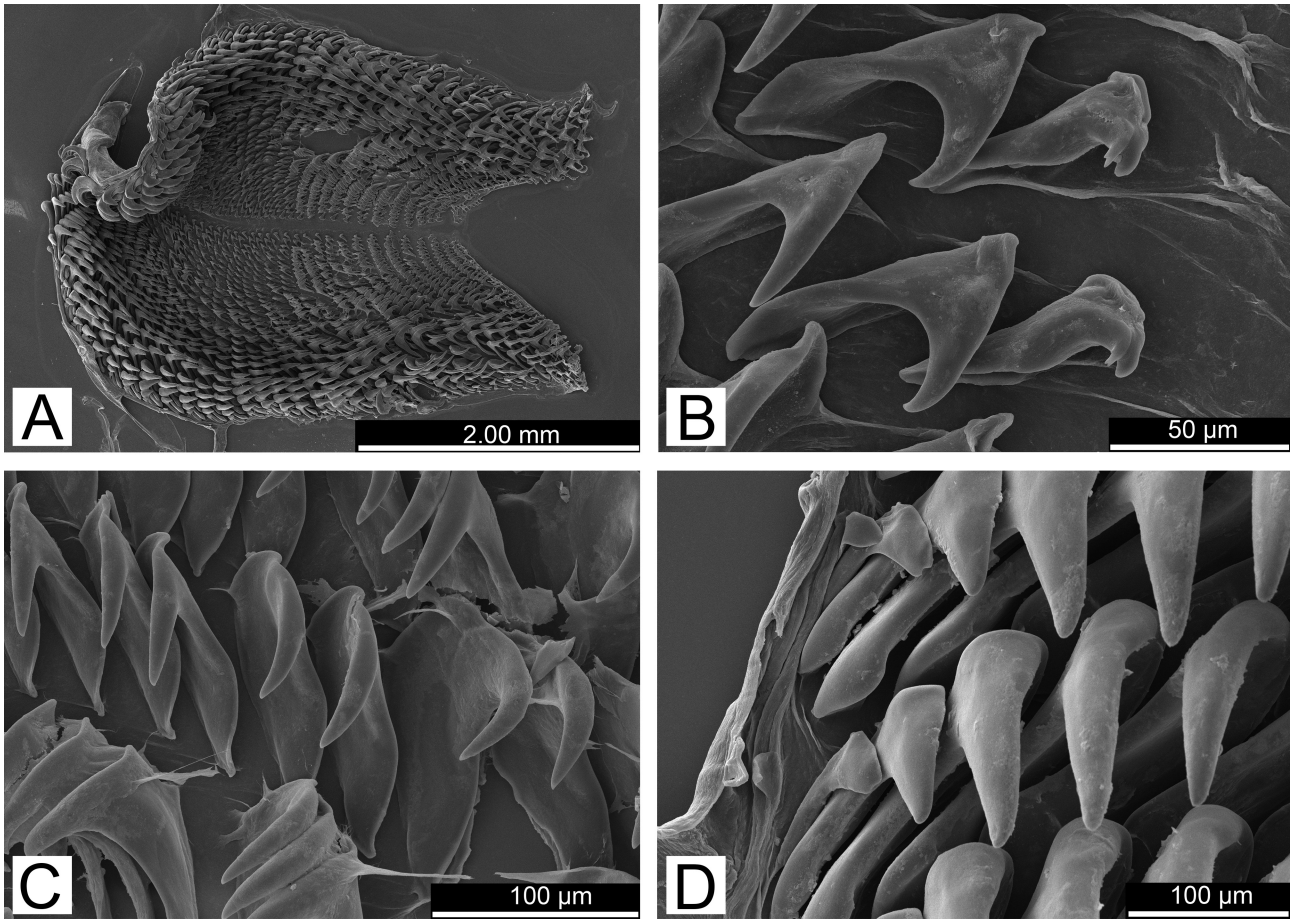

FIGURE 6. *Asteronotus namuro* **sp. nov.** CASIZ 192297. Radula, scanning electron micrographs. **A**. Entire radula; **B**. Central teeth; **C**. Mid-lateral teeth; **D**. Outer lateral teeth.

Geographical distribution. The Saudi Arabian Red Sea.

Remarks. Our molecular phylogeny shows that *Asteronotus namuro* is sister to a clade that includes *A. hepaticus* (Fig. 2E) and *A. cespitosus* (Fig. 2F). The ABGD and bPTP analyses within the clade supports *A. namuro* as a distinct species since there is a minimum divergence of 16.60% between *A. hepaticus* and *A. namuro*, as well as a minimum divergence of 14.55% between *A. cespitosus* and *A. namuro* for the COI gene. Due to the unavailability of additional specimens, intra-specific variation is not studied here; however, *A. namuro* is supported as a distinct species based on the strong external and internal morphological differences combined with the large genetic divergence

between sister taxa. Externally, the body coloration of *A. namuro* is a pinkish pale red with red blotches and numerous red and white tubercles; whereas, *A. hepaticus* is a uniformly dark red color with scattered, minute tubercles, and *A. cespitosus* varies in color from yellow to various shades of brown and red with large irregular tubercles that may be fused together in groups (Valdés & Gosliner 2001, fig. 1A).

The radula and reproductive system of *A. hepaticus* are undescribed and the holotype unavailable for morphological study. Furthermore, the reproductive system of the *A. hepaticus* specimen used in this study could not be reliably described. Therefore, no internal comparisons were made between *A. hepaticus* and *A. namuro*. The radular teeth in *A. namuro* are similar to all *Asteronotus*; however, there is a single triangular denticle on the first tooth in the inner lateral teeth and the outermost tooth is a reduced version of the rest of the outer lateral teeth. In contrast, none of the radular teeth in *A. cespitosus* have denticles and the outermost tooth is elongate rather than simply reduced or an ovoid plate (Valdés & Gosliner 2001, fig. 4). The reproductive system also varies as *A. namuro* has a larger, rounded bursa copulatrix with a smaller ovoid prostate and an irregularly shaped receptaculum seminis; whereas, *A. cespitosus* has a bursa copulatrix and prostate of a similar size with a smaller rounded receptaculum seminis (Valdés & Gosliner 2001, fig. 3B). Additionally, the accessory gland in *A. namuro* is elongate and irregular with a slightly curved accessory spine; whereas, *A. cespitosus* has a more regular shaped accessory gland with a thin, straight accessory spine (Valdés & Gosliner 2001, fig. 5E).

Genus *Hoplodoris* Bergh, 1880

Type species: *Hoplodoris desmoparypha* Bergh, 1880. Formerly in synonymy with *Doris raripilosa* Abraham, 1877, based on morphology (Dayrat 2010); but now removed from synonymy due to a lack of morphological detail or molecular data for *Doris raripilosa*.

Diagnosis. Body covered with simple, rounded tubercles and/or complex branching tubercles; both stiffened with spicules. Broad foot, anteriorly notched. Labial cuticle armed with jaw rodlets. Radula composed of simple, hamate teeth with varying denticulation. Reproductive system composed of a granular prostate with two differentiated sections. Vagina unarmed. Penis armed with hooks. Granular accessory gland armed with an accessory spine (Valdés 2002). Head with two flat oral tentacles (present study).

Hoplodoris desmoparypha Bergh, 1880
(Figs. 7A, 8A, 9, 10A, 11A–B)

Hoplodoris desmoparypha Bergh, 1880:51–56, plate C, figs 5–9, plate F, figs 1–18. Bergh, 1905:113–115, plate XIV, figs 41–46, plate XV, figs 1–2. White, 1950: 99–100.
Asteronotus raripilosa—Dayrat 2010: 174–186, figs 191D–F, 192B, 197F, 200B, 202C, 203B.

Material examined. CASIZ 309550, one specimen, dissected, foot subsampled for molecular analyses, Ngermutidech, 7.31233° N 34.5187° E, Koror Island, Palau, 1m depth, 22 May 1996, Coral Reef Research Foundation. CASIZ 70066, one specimen, foot subsampled for molecular analyses; this specimen was dissected by Dayrat (2010) prior to the present study and re-identified as *Asteronotus raripilosa* by B. Dayrat. Seragaki Beach, 26.50667° N 127.87667° E, Maeki-zaki, Okinawa, Ryukyu, Japan, 25 Feb 1989, R.F. Bolland.

External morphology. The living animals (Fig. 7A) are oval in shape, approximately 55 mm in length, and found along exposed sand bars during low tide at approximately 1m in depth. The body color is tan with random irregularly shaped darker brown spots; numerous light-brown papillae with a few short random branches along a single stem; light-brown and reddish-brown tubercles (Fig. 8A); an irregular white patch along the gill pocket; and irregular dark brown blotches along the center and edge of the mantle. The underside of the mantle is tan with small to medium brown blotches surround the foot. Around the brown blotches are random dark brown flecks. A wide band of light brown specks in semi-irregular patches is offset from the mantle's edge. The gill surrounds the anus and consists of six purplish-brown tripinnate branchial leaves with purplish-brown rachis and light brown tips. The gill pocket contains six lightly crenulated lobes with similar coloration to the rest of the body, as well as numerous papillae. The rhinophores are perfoliate with 15–20 light-brown lamellae with scattered brown spots. The two rhino-

phoral sheaths are irregularly crenulated with similar coloration and papillae to the gill pocket and body. The foot is broad, anteriorly notched, with tan coloration and numerous brown flecks. Flat, slightly rounded triangular-shaped oral tentacles are present laterally on either side of the labial region and mouth.

Internal morphology. *Buccal mass and radula.* The buccal mass is muscular and anteriorly connects to a thin labial cuticle which has semi-elongate jaw rodlets (Fig. 9A). The radula is composed of predominantly hamate teeth and the radular formula is 39 × 61.0.61 in the specimen CASIZ 309550. The inner lateral teeth (Fig. 9B) are short with a broad base and a curved cusp. Some of the inner teeth have one to two triangular denticles on the outer edge of the cusp. The middle lateral teeth (Fig. 9C) are larger with a broader base and more elongate cusp with one to three triangular denticles present on the outer edge of most teeth. The outer lateral teeth (Fig. 9D) are also large, but have a much shorter, rounder cusp than the middle lateral teeth; however, the outermost two teeth are reduced and semi-fimbriate. Most of the outer lateral teeth have one to three denticles on the outer edge of the cusp.

Reproductive system. Due to immature size, the reproductive system of the dissected specimen CASIZ 309550 is small and semi-underdeveloped; however, the reproductive organs were large enough to identify and tentatively describe. An elongate ampulla quickly narrows into the vas deferens and a short oviduct (Fig. 10A). The vas deferens enter the prostate, which expands into an elongate, muscular ejaculatory portion that narrows distally into the penis which shares a common genital atrium with the vagina and accessory gland. The penis is armed with numerous conical penial spines which have an irregular lightly scalloped edge (Fig. 11A). A narrow, elongate vagina enters an irregular, but spherical-shaped bursa copulatrix. A short duct connects near the base of the bursa to a much smaller receptaculum seminis. The uterine duct connects to the base of receptaculum and enters the female gland mass. An ovate, semi-irregular accessory gland is connected to the common genital atrium by a narrow, elongate duct. Within the base of the accessory gland is a slightly curved, but under-developed accessory spine with a semi-broad base (Fig. 11B).

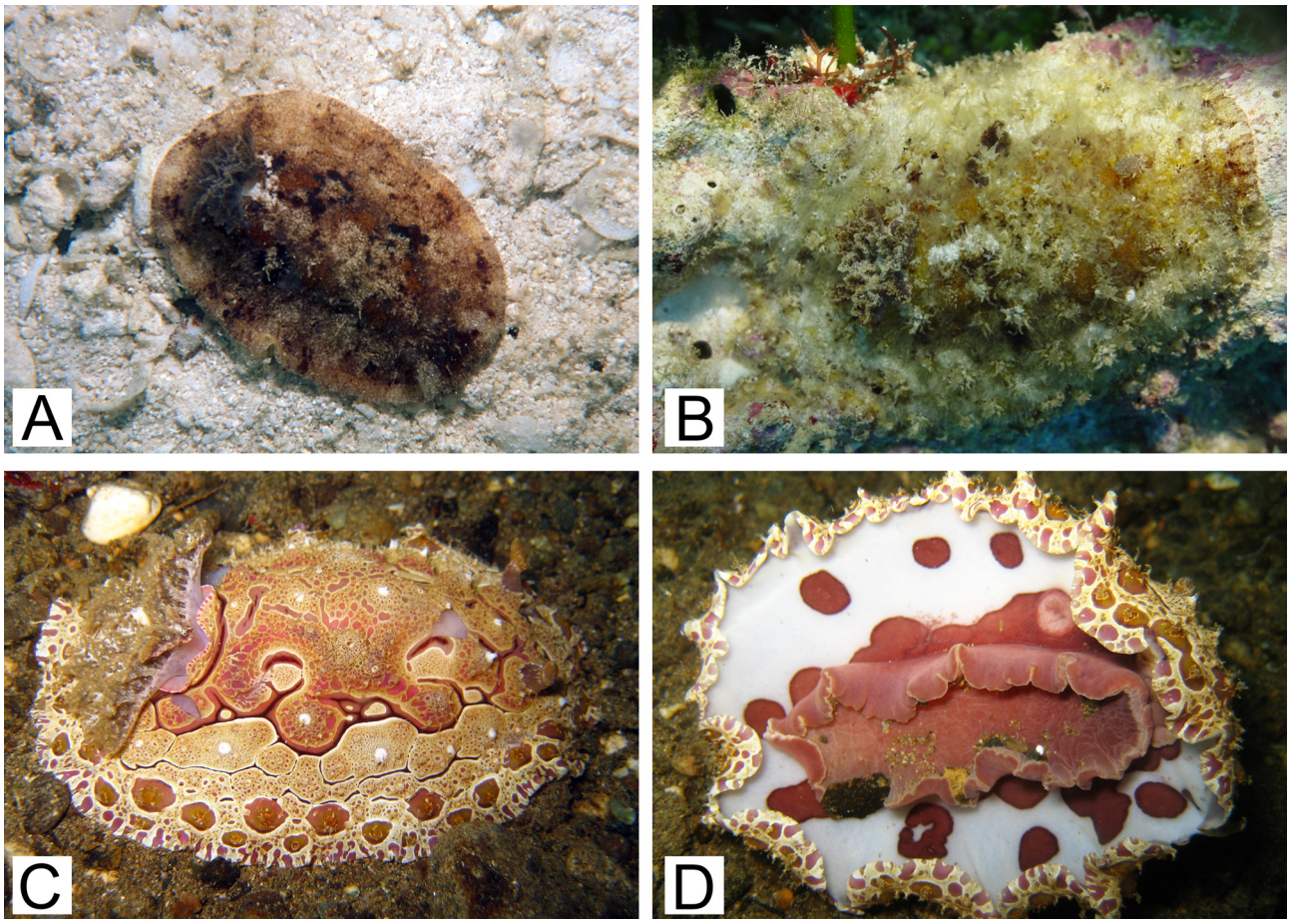

FIGURE 7. *Hoplodoris*, living specimens. **A**. *Hoplodoris desmoparypha* CASIZ 309550, Palau; **B**. *Hoplodoris balbon* **sp. nov.** CASIZ 171406, Philippines; **C**. *Hoplodoris rosans* **sp. nov.** CASIZ 182837, Philippines, dorsal view; **D**. *Hoplodoris rosans* **sp. nov.** CASIZ 182837, Philippines, ventral view. Photos: (A, by Coral Reef Research Foundation), (B, by Marina Poddubetskaia), and (C–D, by Terry Gosliner).

Geographical distribution. Palau (Bergh, 1880) to Indonesia (Bergh, 1905).

Remarks. Our molecular phylogeny, the ABGD analysis, and the bPTP analysis show that *H. desmoparypha* is a distinct species separated from *Asteronotus* by a divergence of 16.47–21.01% with intraspecific variation of 0.16% difference in the COI gene between specimens from the type locality of Palau and a specimen from Japan. Externally, the body coloration of living *H. desmoparypha* from the type locality of Palau was not described by Bergh (1880), but there is some variation in body color between living specimens from Palau and those from Japan studied here. *Hoplodoris desmoparypha* from Palau (CASIZ 309550) has a tan body color with various irregularly shaped brown and white patches, while the individual from Japan (CASIZ 70066) has a white body color and dark brown irregularly shaped patches. The tubercles and papillae are supported by a network of spicules as noted by Bergh (1880, plate F, fig. 18) and the shape of both are similar between specimens; however, the number of retained papillae post preservation varies between specimens (Dayrat 2010, figs. 191D–F). The oral tentacles, gills, and rhinophores are also similar between specimens; but, the younger CASIZ 309550 has fewer rhinophoral lamellae. The radular teeth in CASIZ 309550, closely resemble the size and shape of the radular teeth illustrated in Bergh (1880, plate F, figs. 1–4); however, Bergh's illustrations are missing the triangular denticles found along most of the middle and outer lateral teeth, as well as the semi-fimbriate nature of the outermost tooth. Since CASIZ 309550 is immature, the radular formula was only 39 × 61.0.61; while, in the larger, adult *H. desmoparypha* the radular formula was 50 × 90.0.90 in the specimen CASIZ 70066 (Dayrat 2010, fig. 197F).

The reproductive system in CASIZ 309550 is slightly reduced and underdeveloped. The relative size and shape of the various parts of the system still resemble the reproductive system drawn and described for *H. desmoparypha* in Bergh (1880) and for the adult specimen CASIZ 70066 in Dayrat (2010, fig. 200B). The ampulla studied here is not as long, convoluted, or looped as seen in Dayrat (2010). The prostate is also not as well differentiated into the two distinct sections as seen in the adult CASIZ 70066, which has resulted in a highly elongated prostate. The penial spines in CASIZ 309550 largely resemble the spines described by Bergh (1880, plate F, figs. 8–9) as well as the SEM micrographs of CASIZ 70066 (Dayrat 2010, fig. 202C); however, due to desiccation and perhaps the immature size of the individual the spines have not perfectly retained their conical shape and therefore do not exactly match the drawings and description in Bergh (1880) and Dayrat (2010). The bursa copulatrix studied here is large and rounded and more closely resembles the one found in Bergh (1880, plate F, fig. 5), than the bean-shaped one found in Dayrat (2010, fig. 200B). The accessory gland is similar in shape to the accessory gland for CASIZ 70066 (Dayrat 2010, fig. 200B) and for Bergh's original drawings (Bergh 1880, plate F, fig. 5); however, the accessory spine studied here has a narrower base. In Bergh's original drawings, the accessory spine has a broad base with a curved cusp and a narrow tip (Bergh 1880, plate F, figs. 12–14), as does the specimen CASIZ 70066 (Dayrat 2010, fig. 203B); while CASIZ 309550 is immature resulting in an under-developed accessory spine which has not achieved the expected length, breadth or curvature and more closely resembles the smaller specimen illustrated by Dayrat (2010, fig. 203D for CASIZ 109748 #3).

There is little doubt that the material studied here from Palau and Japan represent a single species. The morphological similarities and the molecular analyses confirm that the Japanese specimen (CASIZ 070066) is conspecific with the specimen from Palau (CASIZ 309550). The geographical distribution of *H. desmoparypha* is poorly understood within the Indo-Pacific, but specimens have been documented in Palau Bergh (1880) and Indonesia (Bergh 1905) with distribution from at least Palau to Japan confirmed here.

Hoplodoris balbon sp. nov.

(Figs. 7B, 8B, 10B, 11C–D, 12)

urn:lsid:zoobank.org:act:F6B9A2AD-2DC5-46C1-A2F8-DE55407BFB84

Type material. **Holotype**: CASIZ 171406, one specimen, dissected, Balicasag Island, 9.51833° N 123.69167° E, Panglao, Bohol Island, Philippines, 4m depth, 25 June 2004, T.M. Gosliner, Y. Camacho-Garcia, J. Templado, M. Malaquias, and M. Poddubetskaia.

Type locality. Balicasag Island, Panglao, Bohol Island, Philippines.

External morphology. The living animals (Fig. 7B) are oval in shape, approximately 40–50 mm in length, and found along coral reefs at 4m in depth. The body color is tan with random brown flecks; numerous light brown and tan papillae with random elongate branches along a single stem; large, complex light brown and reddish-brown tu-

bercles (Fig. 8B); and random white and dark brown blotches along the center and edge of the mantle. The underside of the mantle is tan with small to medium dark brown spots surrounding the foot. A wide band of brown scattered flecks that decrease in density towards the foot is offset from the mantle's edge. The gill consists of six tan tripinnate branchial leaves that surround the anus with dark brown rachises and scattered light brown tips with opaque white spots. The gill pocket contains six lightly crenulated lobes with tan body coloration and numerous papillae. A large white spot is found anterior to the gill pocket. The rhinophores are perfoliate with 25–35 reddish-brown lamellae with scattered opaque white flecks. The two rhinophoral sheaths are lightly crenulated with similar coloration to the gill pocket and body. The foot is broad, anteriorly notched, and tan in color with numerous brown flecks across the whole foot. Flat, slightly rounded oral tentacles are present laterally on either side of the labial region and mouth.

Internal morphology. *Buccal mass and radula.* The buccal mass is muscular and anteriorly connects to a thin labial cuticle, which has elongated jaw rodlets, some of which have a rounded apex and others with a more irregular tip (Fig. 12A). The radula is composed of predominantly smooth hamate teeth and the radular formula is 36 × 66.0.66 in the holotype CASIZ 171406. The inner lateral teeth (Fig. 12B) are short with a broad base and a strongly curved cusp. Some of the first 34 inner teeth have one to three triangular denticles along the outer side of the cusp. The middle lateral teeth (Fig. 12C) are larger and more elongate with a smooth, narrow cusp. The outer lateral teeth (Fig. 12D) are also larger and elongate, but have a slightly shorter, rounder smooth cusp than the middle lateral teeth; however, the two outermost teeth are reduced and semi-fimbriate.

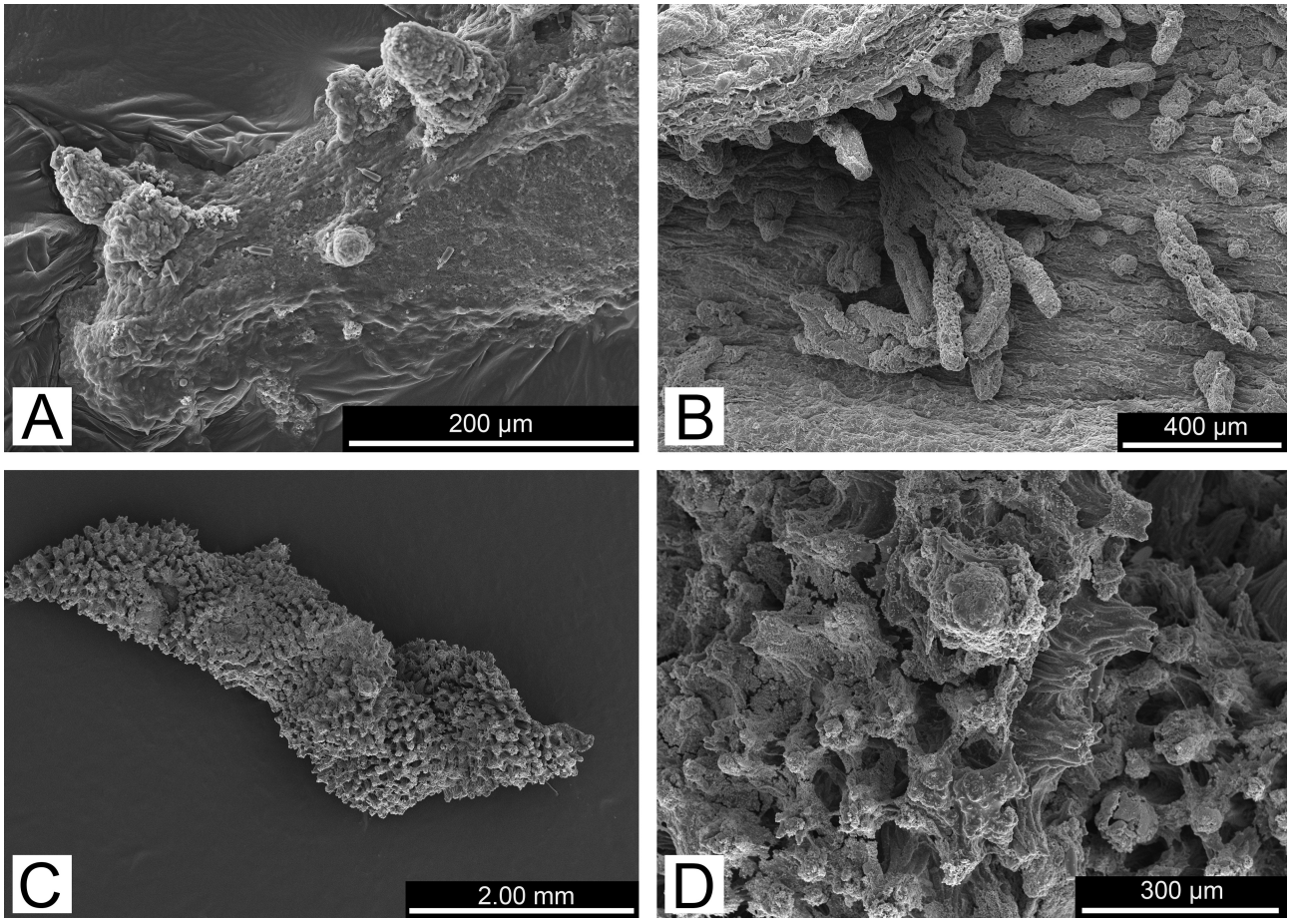

FIGURE 8. *Hoplodoris.* Tubercles and papillae, scanning electron micrographs. **A**. *Hoplodoris desmoparypha* CASIZ 309550; **B**. *Hoplodoris balbon* **sp. nov.** CASIZ 171406. **C–D**. *Hoplodoris rosans* **sp. nov.** CASIZ 182921.

Reproductive system. An elongate ampulla loops and then abruptly narrows into the vas deferens and a short oviduct (Fig. 10B). The vas deferens expands into the rounded portion of the prostate, which then narrows distally into a short, muscular ejaculatory duct and expands again into the bulbous penis that shares a common genital atrium with the accessory gland. The penis is armed with numerous stubby, conical-shaped penial spines with scalloped edges that are attached to a fleshy stem (Fig. 11C). An elongate, narrow vagina enters an irregular bursa copulatrix that is smaller than the prostate and connects to the base of the accessory gland. A short duct connects near the base

of the bursa to a small, ovate receptaculum seminis. A short uterine duct connects to the base of the receptaculum and enters the female gland mass. An irregular-shaped nodular accessory gland is connected to the common genital atrium by a narrow, elongate, convoluted duct. Within the base of the accessory gland is a large, slightly curved accessory spine with a semi-broad base attached to a fleshy stem (Fig. 11D).

Etymology. This species is named *Hoplodoris balbon* after the Filipino word for hairy i.e. "balbon" due to the large, compound tubercles covering the mantle.

Geographical distribution. Known only from Panglao, Philippines.

Remarks. Due to the original preservation in formalin, molecular sequencing of the holotype of *H. balbon* (CASIZ 171406) was unsuccessful for all genes studied; however, the morphological characteristics are sufficiently distinct to distinguish *H. balbon* as a new species within *Hoplodoris*. Externally, the body coloration of *H. balbon* is tan with numerous complex light brown and reddish-brown tubercles, and light brown compound papillae, while *H. desmoparypha* is either cream or white in coloration with brown to dark brown irregular blotches, light brown to reddish brown tubercles, and light brown papillae. The presence of a unique white spot anterior to the gill also appears to be distinctive. The number of gills is similar between species, but the coloration of the leaves and rachis varies. In *H. balbon* the branchial leaves are tan with dark brown rachis and light brown tips, while in *H. desmoparypha* the branchial leaves are purplish-brown with purplish-brown rachis and light brown tips. The coloration of the rhinophores is similar; however, the lamellae in *H. balbon* are more reddish-brown then those in *H. desmoparypha*.

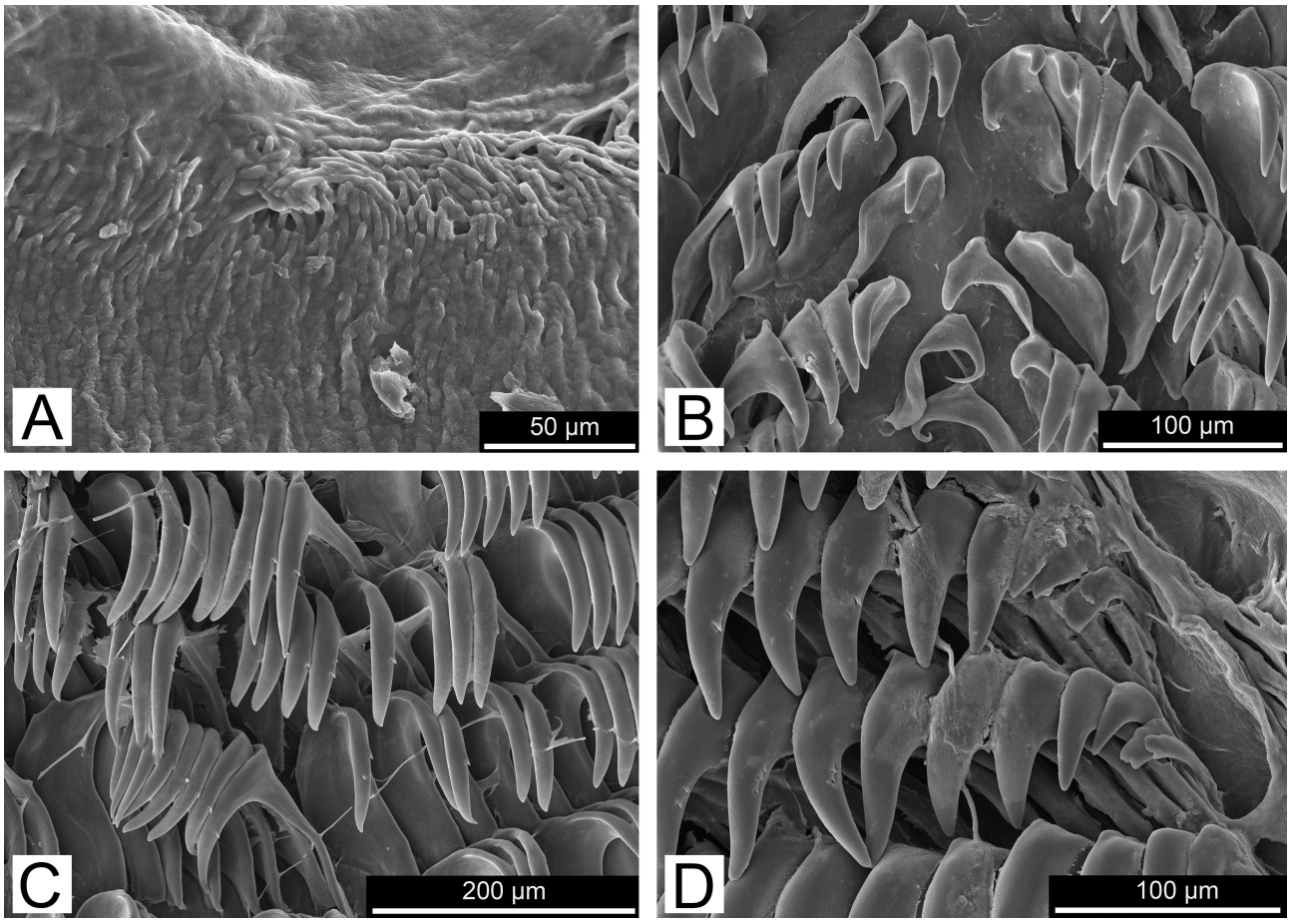

FIGURE 9. *Hoplodoris desmoparypha* CASIZ 309550. Radula, scanning electron micrographs. **A**. Jaw rodlets; **B**. Central teeth; **C**. Mid-lateral teeth; **D**. Outer lateral teeth.

The jaw rodlets are also similar between *H. balbon* and *H. desmoparypha*, but, the rodlets in *H. balbon* are much more elongate with either rounded or irregular tips. The radular teeth in *H. balbon* and *H. desmoparypha* are mostly similar in shape and size; however, the presence and consistency of denticles and the shape of the inner lateral teeth vary between the species. In *H. balbon* the inner lateral teeth have a small base, but a much more elongate cusp then the larger inner lateral teeth in *H. desmoparypha* (Bergh 1880, plate F, figs. 1–2). Denticles are

found along some of the inner lateral teeth in both *H. balbon* and *H. desmoparypha*; while, only *H. desmoparypha* has denticles on the middle and outer lateral teeth. The shape of the outermost tooth in *H. balbon* is also similar to the outermost tooth found in *H. desmoparypha* i.e. reduced and semi-fimbriate (Bergh 1880, plate F, fig. 4). The reproductive system of *H. balbon* has a semi-large rounded prostate armed with conical penial spines elevated on stems, a smaller irregular shaped bursa copulatrix, and a much smaller receptaculum seminis; whereas, *H. desmoparypha* has an irregular prostate which is also armed with conical penial spines, a large rounded bursa copulatrix, and a small receptaculum seminis (Bergh 1880, plate F, fig. 5; Dayrat 2010, fig. 200B). The size and shape of the accessory gland and accessory spine also varies between species. In *H. balbon* the accessory gland is much smaller and elongate on a fleshy base with a slightly curved accessory spine, while *H. desmoparypha* has a slightly larger, more irregularly shaped accessory gland with a broader, curved sessile spine (Bergh 1880, plate F, figs. 5, 12−14; Dayrat 2010, fig. 203B). Though intra-specific variation is not studied here due to the unavailability of additional specimens, *H. balbon* is supported as a distinct species from *H. desmoparypha* based on strong external and internal morphological differences.

***Hoplodoris rosans* sp. nov.**
(Figs. 7C–D, 8C–D, 10C, 11E–F, 13)
urn:lsid:zoobank.org:act:A1EEE912-A939-418E-B7F3-0E738D1B6CA1

Otinodoris sp. 1—Gosliner *et al.* 2008: page 174, second photograph from the bottom. Gosliner *et al.* 2015: page 182, middle right photograph. Gosliner *et al.* 2018: page 103, top left photograph.

Type material. **Holotype**: CASIZ 182921, one specimen, dissected, foot subsampled for molecular analyses, Basura, 13.65648° N 120.91869° E, Mabini (Calumpan Peninsula), Batangas Province, Luzon Island, Philippines, May 2010, Mike Miller. **Paratypes:** CASIZ 182837, one specimen, foot subsampled for molecular analyses, Arthur's Rock, 13.70775° N 120.87481° E, Maricaban Strait, Mabini (Calumpan Peninsula), Batangas Province, Luzon Island, Philippines, 14.6m depth, 20 May 2010, Alicia Hermosillo. CASIZ 105692, one specimen. North Side of Mindoro Island, 13.52657° N 120.95817° E, Philippines, 28 February 1995, T.M. Gosliner.

Type locality. Basura, Mabini (Calumpan Peninsula), Batangas Province, Luzon, Philippines.

External morphology. The living animals (Figs. 7C–D) are large, oval in shape, range in length between 80–120 mm, and are found along reef slops between 12–15m, where they are nocturnally active. The body color is cream and tan with brown papillae with short random branches along a single stem; numerous large tubercles (Figs. 8C–D); pink, red, and light purple concavities along the center; tan and cream concavities in descending size (medium–small) approaching the edge of the mantle; with some concavities lined with black rings, and small purple blotches along the mantle rim. The underside of the mantle is cream with medium rose-colored spots along the edge, large rose-colored blotches surrounding the foot and a light purple band around the mantle's edge. The gill consists of six pale violet tripinnate branchial leaves, light brown rachises with scattered opaque white spots, and surround the anus. The gill pocket contains six distinct lobes with a ring of light pink spots around the edge and patterning like the rest of the body. The rhinophores are perfoliate with 30–45 reddish lamellae. The base and middle regions are brown with some opaque white spots towards the middle region, lower lamellae, and apex. The two rhinophoral sheaths are lightly crenulated with similar body coloration. The foot is broad and reddish purple in color with a tan line along the edge and notched anteriorly. A flat, slightly rounded triangular oral tentacle is present laterally on either side of the labial region and mouth.

Internal anatomy. *Buccal mass and radula.* The buccal mass is muscular and anteriorly connects to a thin labial cuticle which has reduced jaw rodlets (Fig. 13A). The radula is composed of predominantly smooth hamate teeth and the radular formula is 42 × 116.0.116 in the holotype CASIZ 182921. The inner lateral teeth (Fig. 13B) are short with a broad base and a strongly curved cusp. The first 21 inner teeth have one to four triangular denticles along the outer side of the cusp. The middle lateral teeth (Fig. 13C) are slightly larger and more elongate with a narrow cusp and no denticles. The outer lateral teeth (Fig. 13D) also lack denticles but are larger and more elongate than the middle lateral teeth with a slightly rounder smooth cusp.

Reproductive system. An elongate, convoluted ampulla expands and loops before narrowing into the vas deferens and a short oviduct (Fig. 10C). The vas deferens expands and enters a large, spherical prostate that quickly narrows distally into a long convoluted ejaculatory portion. The ejaculatory portion widens again before expanding

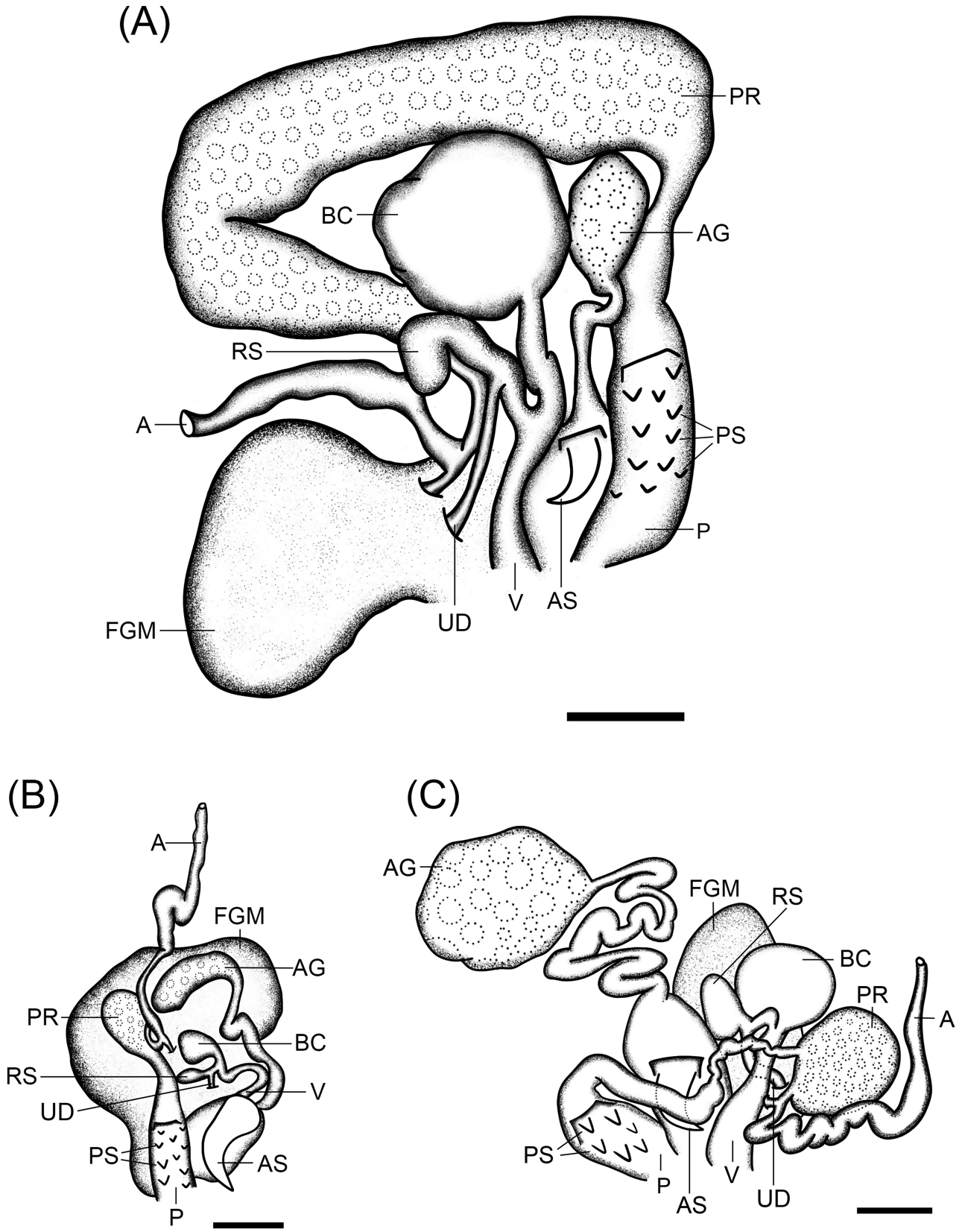

FIGURE 10. *Hoplodoris*, reproductive system. **A**. *Hoplodoris desmoparypha* CASIZ 309550, (scale bar = 0.5mm); **B**. *Hoplodoris balbon* **sp. nov.** CASIZ 171406 (scale bar = 1mm); **C**. *Hoplodoris rosans* **sp. nov.** CASIZ 182921 (scale bar = 2mm). Abbreviations: A, ampulla; AG, accessory gland; AS, accessory spine; BC, bursa copulatrix; FGM, female gland mass; P, penis; PR, prostate; PS, penial spines; RS, receptaculum seminis; UD, uterine duct; V, vagina.

into a muscular, penial bulb that enters the common genital atrium shared with the vagina and accessory gland. The penis is armed with numerous penial spines (Fig. 11E), which have a broad base and are slightly curved at the tip. The broad short vagina narrows as it enters the large, spherical bursa copulatrix. A short, duct connects near the base of the bursa to a smaller, ovoid receptaculum seminis. The uterine duct also connects to the base of the receptaculum and enters the female gland mass. A massive nodular accessory gland is connected by a long and convoluted duct that expands into a muscular base that opens into the center of the common genital atrium between the vagina and the penis. Within the base of the accessory gland there is a large, rose-thorn shaped accessory spine with a broad base and a strongly curved narrow cusp (Fig. 11F).

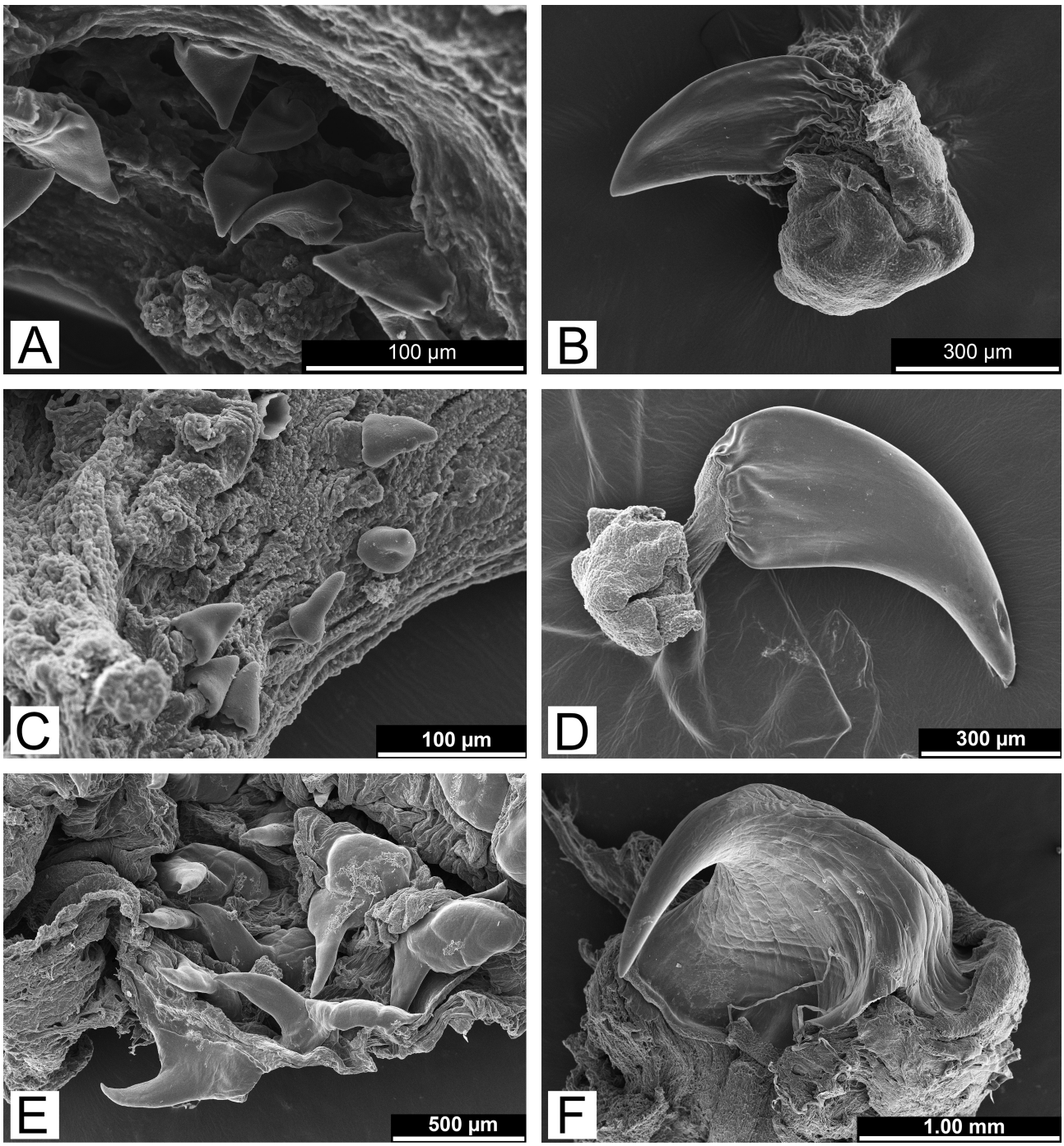

FIGURE 11. *Hoplodoris*, penial and accessory spines, scanning electron micrographs. **A**. *Hoplodoris desmoparypha* CASIZ 309550, penial spines; B. *Hoplodoris desmoparypha* CASIZ 309550, accessory spine; **C**. *Hoplodoris balbon* **sp. nov.** CASIZ 171406, penial spines; **D**. *Hoplodoris balbon* **sp. nov.** CASIZ 171406, accessory spine. **E**. *Hoplodoris rosans* **sp. nov.** CASIZ 182921, penial spines; **F**. *Hoplodoris rosans* **sp. nov.** CASIZ 182921, accessory spine.

Etymology. This species is named *Hoplodoris rosans* after the large rose-colored spots along the underside of the mantle; as well as for the large, rose-thorn shaped accessory spine.

Geographical distribution. The Verde Island Passage of the Philippines.

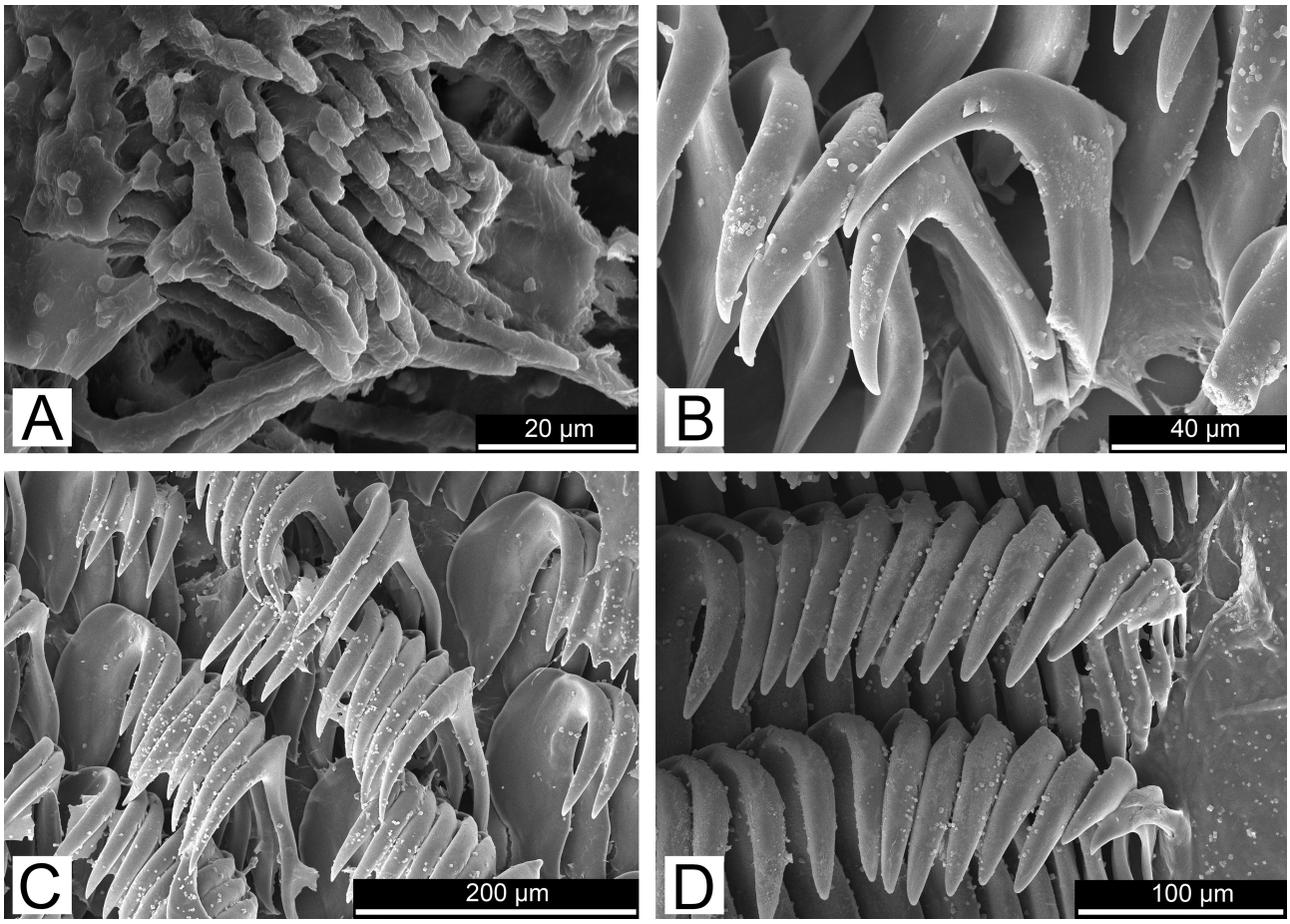

FIGURE 12. *Hoplodoris balbon* **sp. nov.** CASIZ 171406. Radula, scanning electron micrographs. **A**. Jaw rodlets; **B**. Central teeth; **C**. Middle lateral teeth; **D**. Outer lateral teeth.

Remarks. Our molecular phylogeny, the ABGD analysis, and the bPTP analysis show that *H. rosans* is a distinct species within *Hoplodoris* and has a minimum divergence of 15.99% with the type species *H. desmoparypha*. Externally, the body coloration of *H. rosans* is a cream and tan color with large tubercles, colorful concavities ranging from pink to purple, and brown papillae; whereas, *H. balbon* is tan in coloration with reddish-brown compound papillae and light brown tubercles and *H. desmoparypha* is cream or white in color with numerous large brown to dark brown blotches, large light brown and reddish-brown tubercles, and scattered light brown compound papillae. The jaw rodlets in *H. rosans* are vastly different than the rodlets in either *H. balbon* or *H. desmoparypha*. The rodlets found in *H. rosans* are greatly reduced; whereas, the rodlets are semi-elongate in *H. desmoparypha* and extremely elongate in *H. balbon* with rounded or irregular tips. The radular teeth in *H. rosans*. *H. balbon,* and *H. desmoparypha* are similar in shape and size; however, the consistency of denticles and the shape of the outermost tooth vary between the species. In *H. rosans* all of the first 21 inner teeth have denticles which may vary in number, while in *H. balbon* and *H. desmoparypha* only some of the inner teeth have denticles. *Hoplodoris rosans* and *H. balbon* have no denticles along the middle or outer lateral teeth; however, denticles are present along those teeth in *H. desmoparypha*. The shape of the outermost tooth in *H. rosans* is a reduced version of the rest of the outer lateral teeth; whereas in *H. balbon* and *H. desmoparypha* the outermost tooth is reduced and semi-fimbriate (Bergh 1880, plate F, fig. 4).

The reproductive system of *H. rosans* has a large rounded prostate armed with slightly curved penial spines, a slightly smaller bursa copulatrix, and a small receptaculum seminis, while *H. balbon* also has a large prostate armed with stalked rather than sessile conical penial spines, but a smaller irregular shaped bursa copulatrix, and a much smaller receptaculum seminis. Similarly, *H. desmoparypha* also has sessile conical penial spines and a small receptaculum seminis, but the prostate is more irregular in shape and the rounded bursa copulatrix is much larger in size

(Bergh 1880, plate F, fig. 5; Dayrat 2010, fig. 200B). The size and shape of the accessory gland and accessory spine also varies. In *H. rosans* the accessory gland is much larger, irregularly shaped and has a large, rose thorn shaped accessory spine at the base, while *H. balbon* has a slightly smaller, elongate accessory gland with a smaller lightly curved accessory spine and *H. desmoparypha* has a slightly larger, more irregularly shaped accessory gland with a broader, curved accessory spine (Bergh 1880, plate F, figs. 5, 12−14; Dayrat 2010, fig. 203B).

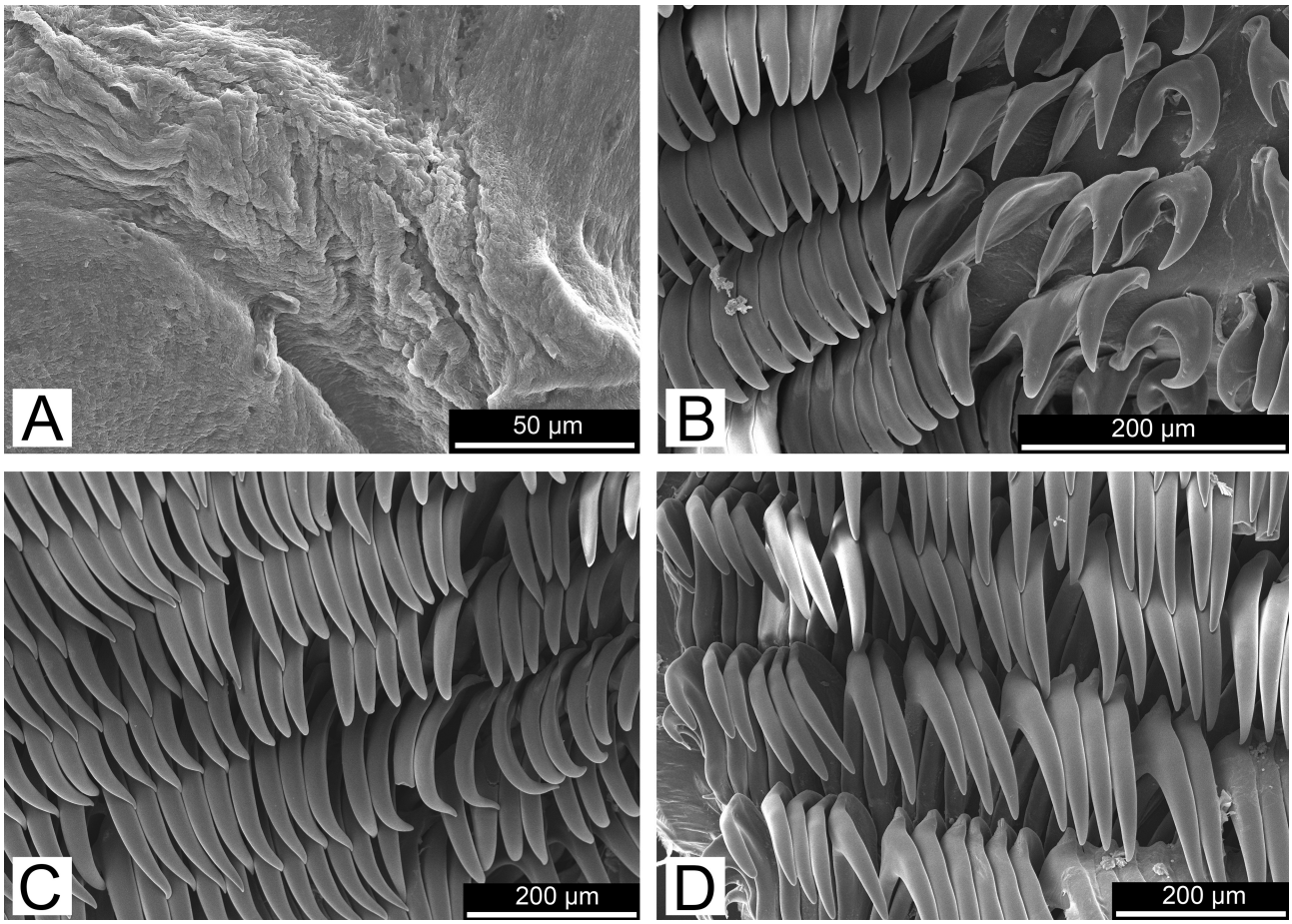

FIGURE 13. *Hoplodoris rosans* **sp. nov.** CASIZ 182921. Radula, scanning electron micrographs. **A**. Jaw rodlets; **B**. Central teeth; **C**. Middle lateral teeth; **D**. Outer lateral teeth.

Discussion

Asteronotus cespitosus has been well studied in several morphological anatomy and systematics studies and is often used for outgroup comparisons during dorid morphological studies (Kay & Young 1970; Edmunds 1971; Valdés & Gosliner 2001; Valdés 2002; Fahey & Garson 2002). *Asteronotus* and *Halgerda* have been frequently grouped together due to a morphological study of caryophyllidia-bearing dorids, which showed that they shared several characteristics including a rigid body with a rubbery texture and a prostate composed of two well-differentiated sections (Valdés & Gosliner 2001). Additionally, Valdés (2002) showed that *Asteronotus* and *Halgerda* also shared some characteristics with *Thordisa* i.e. a smooth labial cuticle devoid of rodlets, and *Hoplodoris* i.e. the presence of one to many hard accessory spines within an accessory gland. The first molecular sequences for *A. cespitosus* demonstrated that *Asteronotus* was more closely related to species of *Halgerda* than to *Peltodoris nobilis* (MacFarland, 1905) (Fahey 2003); however, only one gene (COI) was sequenced and only two other genera from Discodorididae were used for outgroup comparisons. *Asteronotus cespitosus* underwent further revision during a Doridina molecular phylogenetic study, which revealed that *T. albomacula* was the sister taxon of *Asteronotus* rather than *Halgerda* (Hallas *et al.* 2017). To test the phylogenetic estimate of Discodorididae in Hallas *et al.* (2017), we increased the number of outgroup taxa to better reflect the molecular and morphological diversity within Discodorididae. We also obtained molecular sequences for all of the recognized species of *Asteronotus* (*A. cespitosus*, *A. hepaticus*, *A. mi-*

meticus, and *A. spongicolus*) as well as sequences of two new *Asteronotus* species from the Red Sea (*A. markaensis* and *A. namuro*).

Our molecular analyses separate *Asteronotus* into two distinct clades, which appear to be differentiated by coloration and biology rather than biogeography; however, further study is needed to evaluate this relationship. The first clade, including the type species *A. cespitosus*, *A. hepaticus*, and *A. namuro*, is composed of larger species which exhibit more vibrant body coloration, larger tubercles, and fewer papillae (Figs. 2D–F). The second clade is composed of cryptic species including *A. markaensis*, *A. mimeticus*, and *A. spongicolus* which show a close resemblance to their prey sponges (Figs. 2A–C). Crypsis occurs in many species of sponge-eating dorids and is documented in nudibranchs from the Eastern and Indo-Pacific, the Mediterranean Sea, and the southwestern Atlantic (Gosliner & Behrens 1990; Valdés *et al.* 2006; Rudman & Bergquist 2007; Penney 2013; Belmonte *et al.* 2015). Since some species of *Asteronotus* exhibit variation in color we compared intra-specific variation within *A. cespitosus* and *A. spongicolus*. The boldly colored *A. cespitosus* has very little genetic variation between the Philippines and Papua New Guinea (0.15–0.34%). In contrast, the cryptic *A. spongicolus* shows more genetic diversity over a broader geographical range (0.72–2.44%). Unfortunately, only one specimen of *A. markaensis* was available for this study; however, additional specimens may reflect intra-specific variation similar to *A. spongicolus* since both species exhibit cryptic coloration. Additionally, *A. spongicolus* and *A. markaensis* are externally similar; however, these sympatric species have a strong genetic divergence of 13.01−13.67% and clearly demonstrate that they have strong genetic differences that differentiate them as separate species.

Furthermore, our molecular analyses support *Hoplodoris*, rather than *Thordisa*, as the sister taxon of *Asteronotus*. Morphologically, the two taxa share several physical characteristics including a rigid gelatinous body, large tubercles, hamate radular teeth, a large prostate, and an accessory gland armed with an accessory spine. The key differences that separate *Asteronotus* from *Hoplodoris* include digitiform oral tentacles, an absence of jaw rodlets and an unarmed penis. In contrast, *Hoplodoris* has flat, "ear" or semi-triangular shaped oral tentacles, the presence of jaw rodlets, and a penis armed with distinct penial spines. Several synonymies involving the type species *H. desmoparypha* have been previously suggested but never formerly proposed (Eliot 1906, 1910; White 1950; Dorgan *et al.* 2002). The original description of *P. papillata* in Eliot (1904) closely resembles Bergh's description of *H. desmoparypha* i.e. long hamate teeth, an armed penis, crenulated rhinophoral sheaths, various types of papillae, and numerous minute spots and chocolate blotches along the foot. Eliot initially noted the presence of an accessory gland, but no accessory spine; however, further observations led Eliot (1906) to suggest synonymy after closer examination of more specimens resulted in locating a slightly straighter accessory spine within *P. papillata*. Eliot (1906) also mentioned the lack of labial armature within *P. papillata*, but the jaws may have been overlooked due to their small size in relation to the rest of the radula. In a review of *Platydoris* Bergh, 1877b, Dorgan *et al*. (2002) also noted that *P. papillata* may be a synonym of *H. desmoparypha* due to the large and ramified papillae, but that further revision was required. White (1948) described the genus *Otinodoris* based on *O. winckworthi*, which also shares numerous characteristics with *H. desmoparypha* including a tan body coloration with various brown spots, fine and branched papillae, a crenulated branchial sheath, and an armed penis. However, White misinterpreted the prostate as the hermaphrodite gland and there is no mention of the accessory gland, an accessory spine, or labial armature. There have been no additional specimen collections of *O. winckworthi* since its original description, making its taxonomic position uncertain. Dayrat (2010) synonymized *P. papillata*, and *O. winckworthi* , as well as *Otinodoris* sp. (Coleman 2001; Valdés 2004); *Otinodoris* sp. 1 (Marshall & Willan 1999); *Sebadoris* sp. (Debelius 1996; Ono 1999); *Doridacea,* sp. 3 (Ono 1999); and *Sebadoris* sp. cf. *nubilosa* (Ono 2004) with *D. raripilosa*; however, we suggest that synonymy of these species is uncertain until new specimens from type localities are collected and analyzed molecularly and morphologically. It should be noted that the type locality of *D. raripilosa* is unknown, adding further complexity to differentiation between these species.

Carminodoris was synonymized with *Hoplodoris* after an extensive comparison by Fahey & Gosliner (2003) resulted in several synonymies including *H. desmoparypha* with *C. grandiflora*. It was noted that there were two major differences between their specimens of *H. desmoparypha* and Bergh's description. The first was the presence of minute denticles along the outer edge visible only by high-power scanning electron microscopy and the second was the presence of an armed vagina. The authors state that the armed vagina could have been easily missed by Bergh; however, in Bergh's original drawings and descriptions for *H. desmoparypha* the accessory spine is clearly defined at the end of the accessory gland which shares an atrium with the end of the vagina (Bergh 1880, plate F, fig. 11). The spine described by Bergh has a broad base and a curved tip (Bergh 1880, plate F, figs. 12−14), while

the spine described in Fahey & Gosliner (2003) is straight. Additional differences in the morphology of Palau specimens studied here and those from Fahey & Gosliner (2003) further suggest that *H. desmoparypha* is not a junior synonym of *C. grandiflora* and that the synonymy of *Carminodoris* and *Hoplodoris* was unwarranted. Dayrat (2010) also noted this error and officially separated *Carminodoris* from *Hoplodoris*. Furthermore, Dayrat (2010) synonymized several more species of Discodorididae including *H. desmoparypha* under *D. raripilosa* based on morphological comparisons and an extensive literature review. He also considered *Hoplodoris* to be a synonym of *Asteronotus*; however, our molecular analyses do not support this synonymy. The results of our four-gene molecular phylogeny and the species delimitation analyses clearly show a well-supported distinction between the two genera and we maintain them as distinct genera based on the morphological differences noted below.

Genetically, *H. desmoparypha* from the type locality of Palau, as well as a specimen from Japan studied in Dayrat (2010), is 16.47–21.01% different in its COI gene from all specimens of *Asteronotus* studied here. Morphologically, the holotype *D. raripilosa* and specimens of *H. desmoparypha* described by Bergh are quite similar, but there are a few distinct differences that separate the two species. Bergh (1880) described *H. desmoparypha* with flat, semi-triangularly shaped oral tentacles and a reproductive system that included an accessory gland with an accessory spine and an armed penis (Bergh 1880: 51–56, plate C, figs. 5–9, plate F, figs. 1–18), while Abraham (1877) described the oral tentacles of *D. raripilosa* as "flat, semicrescentic in outline, and pointed forwards and inwards" but left the reproductive system undescribed (Abraham 1877: 257, plate XXIX, figs. 29–30). Dayrat (2010) did note that the reproductive system of the holotype of *D. raripilosa* (NHM 1852.10.7.6) was examined but not drawn as it required destroying some structures, but that "an accessory gland with a coiled spine and an armed penis were found." Since the details of the reproductive structures of the holotype of *Doris raripilosa* remain unknown combined with Dayrat's elaboration of the description of the holotype as having an accessory gland with a curved spine and an armed penis, it is likely that Abraham's type is a species of *Hoplodoris*. In Abraham's drawing of the holotype, there appear to be dense elongate simple papillae that are not evident in the present material we examined from Palau and Japan. We suggest *H. desmoparypha* be removed from synonymy with *D. raripilosa* until more is understood about the variation of the various species of *Hoplodoris*. Dayrat (2010) also depicted two specimens of *Hoplodoris* from the Indian Ocean (CASIZ 099347 and CASIZ 073238) both of which to have color patterns that are quite distinct from that found in specimens in the western Pacific. These two specimens also have differences in the denticulation of the radular teeth and in the shape of the accessory spine and penial spines. Dayrat interpreted these differences as intraspecific variation as there was a tacit assumption that they were conspecific. More likely, these individuals represent distinct species, but the available material is not appropriately preserved for molecular study and we are unable to further explore this hypothesis.

The nudibranch family Discodorididae is notoriously problematic, making specimen collections and species identifications immensely difficult. Prior to the present study, the relationship and synonymy between *Hoplodoris* and *Asteronotus* was proposed due to morphological similarities. Based on our results, we have shown that *Hoplodoris* should be removed from synonymy with *Asteronotus* due to strong morphological and genetic differences. Synonymies based on morphology may not be entirely accurate, but the addition of molecular data may be used to further resolve species relationships within nudibranch genera and families.

Acknowledgements

This work was greatly facilitated by several individuals who helped secure specimens were available for study. We are especially grateful to Mike Berumen (King Abdulah University of Science and Technology), Bob Bolland, Philippe Bouchet (Muséum National d'Histoire Naturelle), Yolanda Camacho-Garcia, Henry Cheney, Pat and Lori Colin (Coral Reef Research Foundation), Ali Hermosillo McKowen, Manuel Malaquias, Michael Miller, Peri Paleracio, Marina Poddubetskaia, Alexis Principe and Jose Templado, Material for some of several of the species studied here were kindly supported by Dr. Philippe Bouchet and supported by the Muséum National d'Histoire Naturelle, Paris. Specifically, The Panglao Marine Biodiversity Project was a joint project of Muséum National d'Histoire Naturelle, Paris (PI: Philippe Bouchet) and University of San Carlos, Cebu City (PI: Danilo Largo), funded by grants from the Total Foundation, the French Ministry of Foreign Affairs, and the Asean Regional Center for Biodiversity Conservation (ARCBC), and operating under a permit from the Philippine Bureau of Fisheries and Aquatic Resources (BFAR). This research was supported by a grant from the National Science Foundation: DEB

1257630 to Terrence Gosliner, Kent Carpenter, Richard Mooi, Luiz Rocha and Gary Williams and REU 1358680 to Richard Mooi, which supported Alessandra Lopez's participation in this project. This collaborative research involved the following partners in the Philippines: former Secretary of Agriculture Proceso J. Alcala; former Philippine Consul General Marciano Paynor and the Consular staff in San Francisco; former Bureau of Fisheries and Aquatic Resources (BFAR) Director Attorney Asis G. Perez; BFAR colleagues, especially Attorney Analiza Vitug, Ludivina Labe; National Fisheries and Research Development Institute (NFRDI) colleagues, especially Director Drusila Bayate and November Romena; U.S. Embassy staff, especially Heath Bailey, Richard Bakewell and Maria Theresa N. Villa; staff of the Department of Foreign Affairs; University of the Philippines (UP) administrators and colleagues including UP President Alfredo Pascual, Vice President Giselle Concepción, Dr Annette Meñez; the staff of the National Museum of the Philippines, especially Dr Jeremy Barns, Anna Labrador and Marivene Manuel Santos. We also thank Jessie de los Reyes, Marites Pastorfide, Sol Solleza, Boy Venus, Joy Napeñas, Peri Paleracio, Alexis Principe, the staff of Atlantis Dive Resort Puerto Galera (especially Gordon Strahan, Andy Pope, Marco Inocencio, Stephen Lamont, P.J Aristorenas), the staff of Lago de Oro Beach Club and Protacio Guest House, May Pagsinohin, Susan Po-Rufino, Ipat Luna, Enrique Nuñez, Jen Edrial, Anne Hazel Javier, Jay-o Castillo, Arvel Malubag and Mary Lou Salcedo. Lastly, our sincere thanks are extended to our fellow Academy and Filipino teammates on the expeditions. All the specimens from the Philippines were collected under our Gratuitous Permits (GP-0077-14, GP-0085-15) from the shallow waters of the municipalities of Mabini, Tingloy, Calatagan and Puerto Galera. This is part of the joint Department of Agriculture-NFRDI-California Academy of Sciences Memorandum of Agreement for the ongoing implementation of the National Science Foundation-funded biodiversity expedition in the Verde Island Passage. The specimens were collected in accordance with the terms and conditions of the gratuitous permit and under the supervision of our partners from BFAR Fisheries Regulatory and Quarantine Division and NFRDI. This research was also supported by a grant from the National Science Foundation: DEB 1856407, Collaborative Research: ARTS: Understanding Tropical Invertebrate Diversity Through Integrative Revisionary Systematics and Training to Terrence Gosliner.

We acknowledge and thank the support of the Dr. Earl H. Myers & Ethel M. Myers Oceanographic & Marine Biology Trust for supporting this project, which is a part of Samantha Donohoo's master's thesis research. We would also like to thank our lab mates in the Gosliner Slug Lab and the staff in the Department of Invertebrate Zoology and the Center for Comparative Genomics at the California Academy of Sciences for all of their help.

References

Abraham, P.S. (1877) Revision of the anthobranchiate nudibranchiate Mollusca, with descriptions or notices of forty-one hitherto undescribed species. *Proceedings of the Zoological Society of London*, 196–269, pls. 27–30.

Alfaro, M.E., Zoller, S. & Lutzoni, F. (2003) Bayes or Bootstrap? A Simulation Study Comparing the Performance of Bayesian Markov Chain Monte Carlo Sampling and Bootstrapping in Assessing Phylogenetic Confidence. *Molecular Biology and Evolution*, 20, 255–266.
https://doi.org/10.1093/molbev/msg028

Angas. G.F. (1864) Description d'espèces Nouvelles appurtenant à plusieurs genres de Mollusques Nudibranches des environs de Port-Jackson (Nouvelle-Galles du Sud), accompagnée de dessins faits d'après nature. *Journal de Conchyliologie*, 3 (12), 43–70.

Baba, K. (1993) Two new species of *Carminodoris* (Nudibranchia: Doridiidae) from Japan. *Venus (Japanese Journal of Malacology)*, 52 (3), 223–233.

Belmonte, T., Alvim, J., Padula, V. & Muricy, G. (2015) Spongivory by nudibranchs on the coast of Rio de Janeiro state, southeastern Brazil. *Spixiana*, 38, 187−195.

Bergh, R. (1877) Malacologische Untersuchungen. *In*: Semper, C. (Eds.), *Reisen im Archipel der Philippinen. Zweiter Theil. Wissenschaftliche Resultate. Band 2. Theil 2. Heft 10*. C. W. Kreidel, Wiesbaden, pp. 495–546.

Bergh, R. (1877b) Kritische Untersuchung der Ehrenberg'schen Doriden. *Deutsche Malakozoologische Gesellschaft Jahrbücher*, 4, 45–76.

Bergh, R. (1878) Malacologische Untersuchungen. *In*: Semper, C. (Eds.), *Reisen im Archipel der Philippinen. Zweiter Theil. Wissenschaftliche Resultate. Band 2. Theil 2. Heft 13 & 14*. C. W. Kreidel, Wiesbaden, pp. 547–601 & 603–645.

Bergh R. (1879) Neue Chromodoriden. *Malakozoologische Blätter Neue Folge*, 1, 87–116.

Bergh, R. (1880) Malacologische Untersuchungen. *In*: Semper, C. (Eds.), *Reisen im Archipel der Philippinen. Zweiter Theil. Wissenschaftliche Resultate. Theil 4. Heft 2*. C. W. Kreidel, Wiesbaden, pp. 1–78, pls. A–F.

Bergh, R. (1880b) Beiträge zur Kenntniss der japanischen nudibranchien. I. *In*: Verhandlungen der Koniglich-Kaiserlichen Zoologisch-Botanischen Gesellschaft in Wien, 30, pp. 155–200.

Bergh, R. (1889) Malacologische Untersuchungen. *In*: Semper, C. (Eds.), *Reisen im Archipel der Philippinen. Zweiter Theil. Wissenschaftliche Resultate. Band 2. Theil 3. Heft 16. 2 Hälfte.* C. W. Kreidel, Wiesbaden, pp. 815–872.
Bergh, R. (1891) Die cryptobranchiaten Dorididen. *Zoologische Jahrbücher, Abteilung für Systematik, Geographie und Biologie der Tiere*, 6, 103–144.
https://doi.org/10.5962/bhl.title.11223
Bergh, R. (1904) Malacologische Untersuchungen. *In*: Semper, C. (Eds.), *Reisen im Archipel der Philippinen. Zweiter Theil. Wissenschaftliche Resultate. Band 9. Theil 6. Heft 1.* C. W. Kreidel, Wiesbaden, pp. 1–56.
Bergh, R. (1905) *Die Opisthobranchiata der Siboga-Expedition. Monographie 50*. E.J. Brill, Leiden, 248 pp.
Burn, R. (1962) Notes on a collection of Nudibranchia (Gastropoda: Doridiidae and Dendrodoridiidae) from South Australia with remarks on the species of Basedow and Hedley, 1905. *Memoirs of the National Museum of Victoria*, 25, 149−171.
https://doi.org/10.24199/j.mmv.1962.25.07
Burn, R. (2006) A checklist and bibliography of the Opisthobranchia (Mollusca: Gastropoda) of Victoria and the Bass Strait area, south-eastern Australia. *Museum Victoria Science Reports*, 10 (142), 7–13.
https://doi.org/10.24199/j.mvsr.2006.10
Chan, J.M. and Gosliner, T.M. (2007) Preliminary phylogeny of *Thordisa* (Nudibranchia: Discodorididae) with descriptions of five new species. *The Veliger,* 48(4): 284–308.
Coleman, N. (2001) *1001 Nudibranchs of the south Pacific. Vol. 1*. Sea Australia Resource Centre, Springwood, 144 pp.
Colgan, D.J., McLauchlan, A., Wilson, G.D.F., Livingston, S.P., Edgecombe, G.D., Macaranas, J., Cassis, G. & Gray, M.R. (1998) Histone H3 and U2 snRNA DNA sequences and arthropod molecular evolution. *Australian Journal of Zoology*, 46 (5), 419−437.
https://doi.org/10.1071/ZO98048
Cooper, J.G. (1863) Some new genera and species of California Mollusca. *Proceedings of the California Academy of Natural Sciences*, 1 (2), 202–207.
Cuvier, G. (1817) Le règne animal distribué d'après son organisation. *In*: *Contenant Les Reptiles, Les Poissons, Les Mollusques, Les Annélides*. *Tome 2.* Deterville, Paris, pp. 351–508, pl. XVIII.
Dayrat, B., Tillier, A., Lecointre, G. & Tillier, S. (2001) New clades of euthyneuran gastropods (Mollusca) from 28S rRNA sequences. *Molecular Phylogenetics and Evolution*, 19, 225–235.
https://doi.org/10.1006/mpev.2001.0926
Dayrat, B. (2010) A monographic revision of basal discodorid sea slugs (Gastropoda, Opisthobranchia, Nudibranchia, Doridina). *Proceedings of the California Academy of Sciences*, Series 4, 61 (1), 1–403, 382 figs.
Debelius, H. (1996) *Nudibranchs and sea snails Indo-Pacific field guide.* IKAN-Unterwasserarchiv, Frankfurt, 321 pp.
Dorgan, K.M., Valdés, Á. & Gosliner, T.M. (2002) Phylogenetic systematics of the genus *Platydoris* (Mollusca, Nudibranchia, Doridoidea) with descriptions of six new species. *Zoologica Scripta*, 31 (3), 271–319.
https://doi.org/10.1046/j.1463-6409.2002.00105.x
Drummond, A.J. & Rambaut, A. (2007) BEAST: Bayesian evolutionary analysis by sampling trees. *BMC evolutionary biology*, 7 (1), 214.
https://doi.org/10.1186/1471-2148-7-214
Edmunds, M. (1971) Opisthobranchiate Mollusca from Tanzania (Suborder: Doridacea). *Zoological Journal of the Linnean Society*, 50, 339–396.
https://doi.org/10.1111/j.1096-3642.1971.tb00767.x
Ehrenberg, C.G. (1828–1831) Symbolae physicae animalia evertebrata exclusis insectis. Series prima cum tabularum decade prima continent animalia Africana et Asiatica. Decas Prima. *In*: Hemprich, F.G. & Ehrenberg, C.G. (Eds.), *Symbolae physicae, seu Icones adhue ineditae corporum naturalium novorum aut minus cognitorum, quae ex itineribus per Libyam, Aegyptum, Nubiam, Dengalam, Syriam, Arabiam et Habessiniam Pars Zoologica, 4*. Officina Academica, Berlin, pls. 1–2 (1828), text (1831). [no pagination]
Eliot, C.N.E. (1904) On some nudibranchs from east Africa and Zanzibar. Part III. Doridiidae Cryptobranchiatae, I. *Proceedings of the Zoological Society of London*, 2, 354–385.
Eliot, C.N.E. (1906) On the nudibranchs of southern India and Ceylon, with special reference to the drawings by Kelaart and the collections belonging to Alder and Hancock preserved in the Hancock Museum at Newcastle-on-Tyne. *Proceedings of the Zoological Society of London*, 1906, 636–691.
Eliot, C.N.E. (1910) Nudibranchs collected by Mr. Stanley Gardiner from the Indian Ocean in H.M.S. Sealark. *In*: Reports of the Percy Sladen Trust Expedition to the Indian Ocean in 1905, under the leadership of Mr. J. Stanley Gardiner, M.A. *Transactions of the Linnean Society, Zoology*, Series 2, 13 (2), 411–439.
https://doi.org/10.1111/j.1096-3642.1910.tb00082.x
Fahey, S.J. (2003) Phylogeny of *Halgerda* (Mollusca: Gastropoda) based on combined analysis of mitochondrial *CO1* and morphology. *Invertebrate Systematics*, 17 (5), 617–624.
https://doi.org/10.1071/IS02048
Fahey, S.J. & Garson, M.J. (2002) Geographic variation of natural products of tropical nudibranch *Asteronotus cespitosus*. *Journal of Chemical Ecology*, 28 (9), 773–1785.
https://doi.org/10.1023/A:1020509117545
Fahey, S.J. & Gosliner, T.M. (2003) Mistaken identities: On the Discodoridiidae genera *Hoplodoris* Bergh, 1880 and *Carminodo-*

ris Bergh, 1889 (Opisthobranchia, Nudibranchia). *Proceedings of the California Academy of Sciences*, 54 (10), 169–208.
Folmer, O., Hoeh, W.R., Black, M.B. & Vrijenhoek, R.C. (1994) Conserved primers for PCR amplification of mitochondrial DNA from different invertebrate phyla. *Molecular Marine Biology and Biotechnology*, 3, 294−299.
Franc, A. (1968) Mollusques, gastéropodes et scaphopodes. *In*: Grassé, P. (Eds.), *Traité de Zoologie Anatomie, Systématique, Biologie. Vol. 5*. Masson, Paris, pp. 608–893.
Giribet, G., Okusu, A., Lindgren, A.R., Huff, S.W., Schrödl, M. & Nishiguchi, M.K. (2006) Evidence for a clade composed of molluscs with serially repeated structures: monoplacophorans are related to chitons. *Proceedings of the National Academy of Sciences*, 103 (20), 7723–7728.
https://doi.org/10.1073/pnas.0602578103
Göbbeler, K. & Klussmann-Kolb, A. (2010) Out of Antarctica?–New insights into the phylogeny and biogeography of the Pleurobranchomorpha (Mollusca, Gastropoda). *Molecular Phylogenetics and Evolution*, 55 (3), 996–1007.
https://doi.org/10.1016/j.ympev.2009.11.027
Gosliner, T.M. & Behrens, D.W. (1990) Special resemblance, aposematic coloration and mimicry in opisthobranch gastropods. Adaptive coloration in invertebrates. *Texas A&M University Sea Grant College Program, College Station*, 1990, 127–138.
Gosliner, T.M. & Behrens, D.W. (1998) Two new Discodorid nudibranchs from the western Pacific with a redescription of *Doris luteola* Kelaart, 1858. *Proceedings of the California Academy of Sciences*, Series 4, 50 (11), 279–293.
Gosliner, T. & Valdés, Á. (2002) Sponging off of Porifera: new species of cryptic dorid nudibranchs (Mollusca, Nudibranchia) from the tropical Indo-Pacific. *Proceedings of the California Academy of Sciences*, 53 (5), 51–61.
Gosliner, T.M., Behrens, D.W. & Valdés, Á. (2008) *Indo-Pacific nudibranchs and sea slugs: a field guide to the world's most diverse fauna*. Sea Challengers, California Academy of Sciences, Gig Harbor, Washington, 426 pp.
Gosliner, T., Behrens, D. & Valdés, Á. (2015) *Indo-Pacific nudibranchs and sea slugs: a field guide to the world's most diverse fauna*. New World Publications, Inc. Jacksonville, Florida, 408 pp.
Gosliner, T.M., Valdeìs, A. & Behrens, D.W. (2018) *Indo-Pacific nudibranchs and sea slugs: a field guide to the world's most diverse fauna*. New World Publications, Inc. Jacksonville, Florida, 451 pp.
Hallas, J.M., Chichvarkhin, A. & Gosliner, T.M. (2017) Aligning evidence: concerns regarding multiple sequence alignments in estimating the phylogeny of the Nudibranchia suborder Doridina. *Royal Society Open Science*, 4 (10), 171095.
https://doi.org/10.1098/rsos.171095
Hasselt, J.C. van (1824) Extrait d'une lettre du Dr. J.C. van Hasselt au Prof. Van Swinderen, sur mollusques de Java, le 25 mai 1823 (I). *Bulletindes Sciences Naturelle et de Géologie*, 3, 237–245.
Kay, E.A. & Young, D.K. (1970) The Doridacea (Opisthobranchia; Mollusca) of the Hawaiian Islands. *Pacific Science*, 23, 172–231.
Katoh, K., Asimenos, G. & Toh, H. (2009) Multiple alignment of DNA sequences with MAFFT. *Methods in Molecular Biology*, 537, 39–64.
https://doi.org/10.1007/978-1-59745-251-9_3
Kearse, M., Moir, R., Wilson, A., Stones-Havas, S., Cheung, M., Sturrock, S., Buxton, S., Cooper, A., Markowitz, S., Duran, C., Thierer, T., Ashton, B., Meintjes, P. & Drummond, A. (2012) Geneious Basic: An integrated and extendable desktop software platform for the organization and analysis of sequence data. *Bioinformatics*, 28, 1647–1649.
https://doi.org/10.1093/bioinformatics/bts199
Kekkonen, M., Mutanen, M., Kaila, L., Nieminen, M. & Hebert, P.D. (2015) Delineating species with DNA barcodes: a case of taxon dependent method performance in moths. *PLoS One*, 10 (4), e0122481.
https://doi.org/10.1371/journal.pone.0122481
Lanfear, R., Frandsen, P.B., Wright, A.M., Senfeld, T. & Calcott, B. (2016) PartitionFinder 2: New Methods for Selecting Partitioned Models of Evolution for Molecular and Morphological Phylogenetic Analyses. *Molecular Biology and Evolution*, 34 (3), 772–773.
https://doi.org/10.1093/molbev/msw260
Lindsay, T., Kelly, J., Chichvarkhin, A., Craig, S., Kajihara, H., Mackie, J. & Valdés, Á. (2016) Changing spots: pseudocryptic speciation in the North Pacific dorid nudibranch *Diaulula sandiegensis* (Cooper, 1863)(Gastropoda: Heterobranchia). *Journal of Molluscan Studies*, 82 (4), 564–574.
https://doi.org/10.1093/mollus/eyw026
MacFarland, F.M. (1905) A preliminary account of the Dorididae of Monterey Bay, California. *Proceedings of the Biological Society of Washington*, 18, 35–54
Maddison, W.P. & Maddison, D.R. (2018) Mesquite: a modular system for evolutionary analysis. Available from: http://mesquiteproject.org/mesquiteArchives/mesquite1.02/mesquite/download/MesquiteManual.pdf (accessed 5 August 2020)
Malaquias, M., Calado, G., Padula, V., Villani, G. & Cervera, J.L. (2009) Molluscan diversity in the North Atlantic Ocean: new records of opisthobranch gastropods from the Archipelago of the Azores. *Marine Biodiversity Records*, 2 (e38), 1−9.
https://doi.org/10.1017/S175526720800016X
Marcus, Ev. & Marcus, Er. (1970) Some gastropods from Madagascar and west Mexico. *Malacologia*, 10 (1), 181–223.
Marshall, J.G. & Willan, R.C. (1999) *Nudibranchs of Heron Island, Great Barrier Reef. A Survey of the Opisthobranchia (Sea Slugs) of Heron and Wistari Reefs.* Backhuys Publishers, Leiden, 268 pp.
Miller, M.C. (1991) On the identity of the dorid nudibranch *Homoiodoris novaezelandiae* Bergh, 1904 (Gastropoda: Opistho-

branchia). *Journal of Natural History*, 25 (2), 293–304.
https://doi.org/10.1080/00222939100770211
Miller, M.A., Pfeiffer, W. & Schwartz, T. (2010) "Creating the CIPRES Science Gateway for inference of large phylogenetic trees". *In*: *Proceedings of the Gateway Computing Environments Workshop (GCE)*, New Orleans, Louisana, 2010, pp. 1–8.
https://doi.org/10.1109/GCE.2010.5676129
MolluscaBase (2020) MolluscaBase. *Asteronotus* Ehrenberg, 1831. Available from: http://www.molluscabase.org/aphia.php?p=taxdetails&id=206528 (accessed 29 July 2020)
Moore, E.J. & Gosliner, T.M. (2011) Molecular phylogeny and evolution of symbiosis in a clade of Indopacific nudibranchs. *Molecular Phylogenetics and Evolution*, 58 (1), 116−123.
https://doi.org/10.1016/j.ympev.2010.11.008
Ono, A. (1999) *Opisthobranchs of Kerama Islands.* TBS-Britannica, Tokyo, 184 pp.
Ono, A. (2004) *Opisthobranchs of Ryukyu Islands*. Rutles, Tokyo, 304 pp.
Ortigosa, D., Pola, M., Carmona, L., Padula, V., Schrödl, M. & Cervera, J.L. (2014) Redescription of *Felimida elegantula* (Philippi, 1844) and a preliminary phylogeny of the European species of *Felimida* (Chromodorididae). *The Journal of Molluscan Studies*, 80, 541–550.
https://doi.org/10.1093/mollus/eyu041
Palumbi, S.R., Martin, A.P., Romano, S., McMillan, W.O., Stice, L. & Grabowski, G. (1991) *The Simple Fool's Guide to PCR*. Department of Zoology, University of Hawaii, Honolulu, 47 pp. [Special Publication]
Pease, W.H. (1860) Descriptions of new species of Mollusca from the Sandwich Islands. *Proceedings of the Zoological Society of London*, 28, 18–37.
Penney, B.K. (2013) How specialized are the diets of northeastern pacific sponge-eating dorid nudibranchs? *Journal of Molluscan Studies*, 79, 64–73.
https://doi.org/10.1093/mollus/eys038
Platt, A.R., Woodhall, R.W. & George, A.L. (2007) Improved DNA sequencing quality and efficiency using an optimized fast cycle sequencing protocol. *BioTechniques*, 43, 58–62.
https://doi.org/10.2144/000112499
Pola, M., Padula, V., Gosliner, T.M. & Cervera, J.L. (2014) Going further on an intricate and challenging group of nudibranchs: description of five novel species and a more complete molecular phylogeny of the subfamily Nembrothinae (Polyceridae). *Cladistics*, 30 (6), 607–634.
https://doi.org/10.1111/cla.12097
Puillandre, N., Lambert, A., Brouillet, S. & Achaz, G. (2012) ABGD, Automatic Barcode Gap Discovery for primary species delimitation. *Molecular Ecology*, 21, 1864–1877.
https://doi.org/10.1111/j.1365-294X.2011.05239.x
Rao, K.V., Sivadas, P. & Kumary, L.K. (1974) On three rare doridiform nudibranch molluscs from Kavaratti Lagoon, Laccadive Islands. *Journal of the Marine Biological Association of India*, 16 (1), 113–125.
Ronquist, F. & Huelsenbeck, J.P. (2003) MrBayes 3: Bayesian phylogenetic inference under mixed models. *Bioinformatics*, 19, 1572–1574.
https://doi.org/10.1093/bioinformatics/btg180
Rudman, W. & Bergquist, P.R. (2007) A review of feeding specificity in the sponge-feeding Chromodorididae (Nudibranchia: Mollusca). *Molluscan Research*, 27, 60–88.
Stamatakis, A. (2014) RAxML version 8: a tool for phylogenetic analysis and post-analysis of large phylogenies. *Bioinformatics*, 30, 1312–1313.
https://doi.org/10.1093/bioinformatics/btu033
Swofford, D. L. (2003) *PAUP*. Phylogenetic Analysis Using Parsimony (*and Other Methods). Version 4*. Sinauer Associates, Sunderland, Massachusetts. [software]
Thompson, T.E. (1975) Dorid nudibranchs from eastern Australia (Gastropoda, Opisthobranchia). *Journal of Zoology*, 176 (4), 477–517.
https://doi.org/10.1111/j.1469-7998.1975.tb03216.x
Thollesson, M. (2000) Increasing fidelity in parsimony analysis of dorid nudibranchs by differential weighting, or a tale of two genes. *Molecular Phylogenetics and Evolution*, 16 (2), 161–172.
https://doi.org/10.1006/mpev.2000.0789
Tibiriçá, Y., Pola, M. & Cervera, J.L. (2019) Systematics of the genus *Halgerda* Bergh, 1880 (Heterobranchia: Nudibranchia) of Mozambique with descriptions of six new species. *Invertebrate systematics*, 32 (6), 388–1421.
https://doi.org/10.1071/IS17095
Valdés, Á. (2002) A phylogenetic analysis and systematic revision of the cryptobranch dorids (Mollusca, Nudibranchia, Anthobranchia). *Zoological Journal of the Linnean Society*, 136, 535–636.
https://doi.org/10.1046/j.1096-3642.2002.00039.x
Valdés, Á. (2004) Morphology of the penial hooks and vaginal cuticular lining of some dorid nudibranchs (Mollusca, Opisthobranchia). *American Malacological Bulletin*, 18, 49–53.
Valdés, Á. & Gosliner, T.M. (2001) Systematics and phylogeny of the caryophyllidia-bearing dorids (Mollusca, Nudibranchia),

with descriptions of a new genus and four new species from Indo-Pacific deep waters. *Zoological Journal of the Linnaean Society*, 133 (2), 103–198.
https://doi.org/10.1111/j.1096-3642.2001.tb00689.x

Valdés, Á., Hamann, J., Behrens, D.W. & Dupont, A. (2006) *Caribbean Sea Slugs.* Sea Challengers, Gig Harbor, Washington, 289 pp.

Wägele, H. & Willan, R.C. (2000) Phylogeny of the Nudibranchia. *Zoological Journal of the Linnean Society*, 130 (1), 83–181.
https://doi.org/10.1111/j.1096-3642.2000.tb02196.x

White, K.M. (1948) On a collection of marine molluscs from Ceylon. *Proceedings of the Malacolgoical Society of London*, 27 (5), 199–205.

White, K.M. (1950) On the nudibranch genera *Platydoris, Artachaea,* and *Hoplodoris. Proceedings of the Malacological Society of London*, 28 (2–3), 93–101.

Xia, Y., Gu, H., Peng, R., Chen, Q., Zheng, Y., Murphy, R.W. & Zeng, X. (2012) COI is better than 16S rRNA for DNA barcoding Asiatic salamanders (Amphibia: Caudata: Hynobiidae). *Molecular Ecology Resources*, 12, 48–56.
https://doi.org/10.1111/j.1755-0998.2011.03055.x

Zhang, J., Kapli, P., Pavlidis, P. & Stamatakis, A. (2013) A general species delimitation method with applications to phylogenetic placements. *Bioinformatics*, 29 (22), 2869–2876.
https://doi.org/10.1093/bioinformatics/btt499

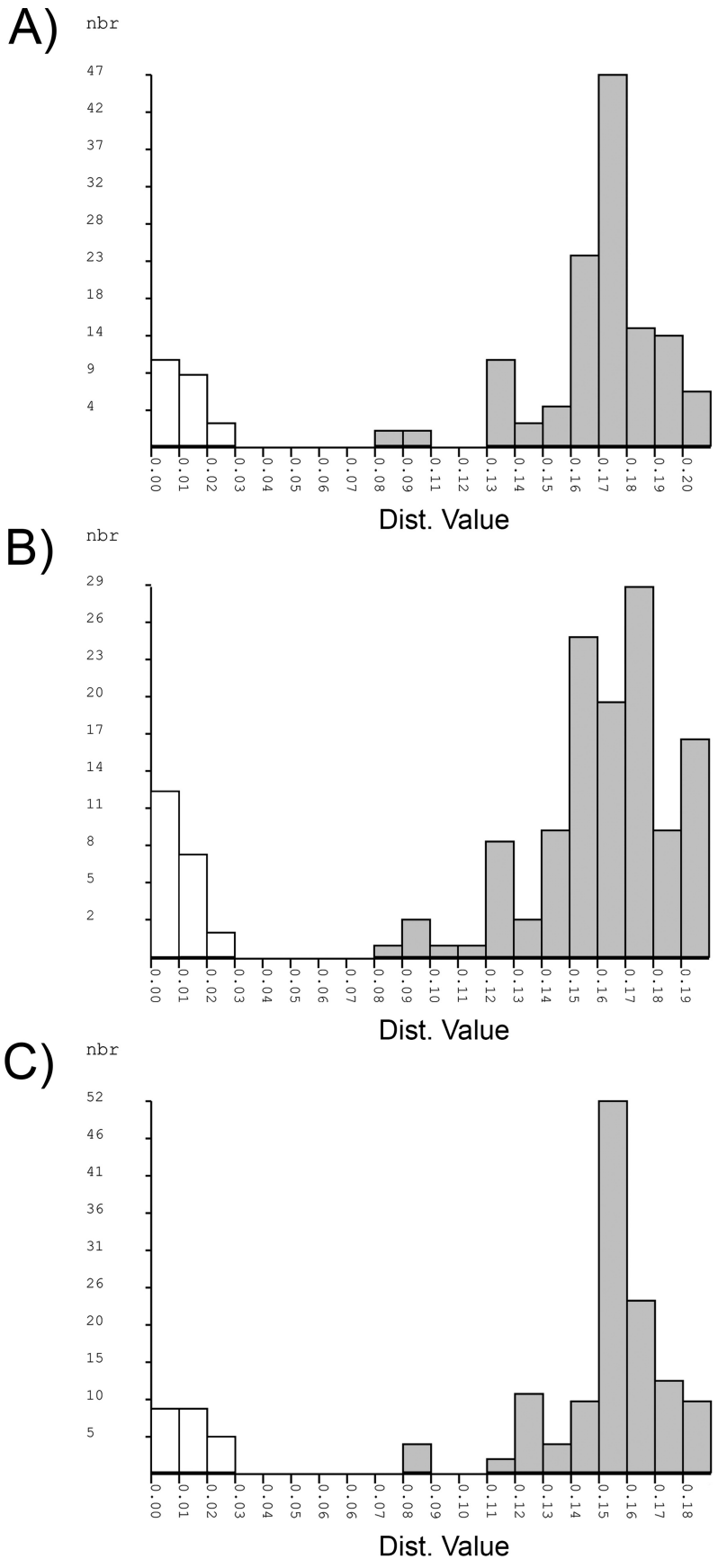

FIGURE S1. Automatic Barcode Gap Discovery genetic distances calculated for 18 *Asteronotus* Ehrenberg, 1831 and *Hoplodoris* Bergh, 1880 COI sequences using three genetic distance calculations: (A) Jukes-Cantor (JC69); (B) Kimura (K80); (C) Simple Distance. Presumed intraspecific variation is shown in white, interspecific variation in grey.

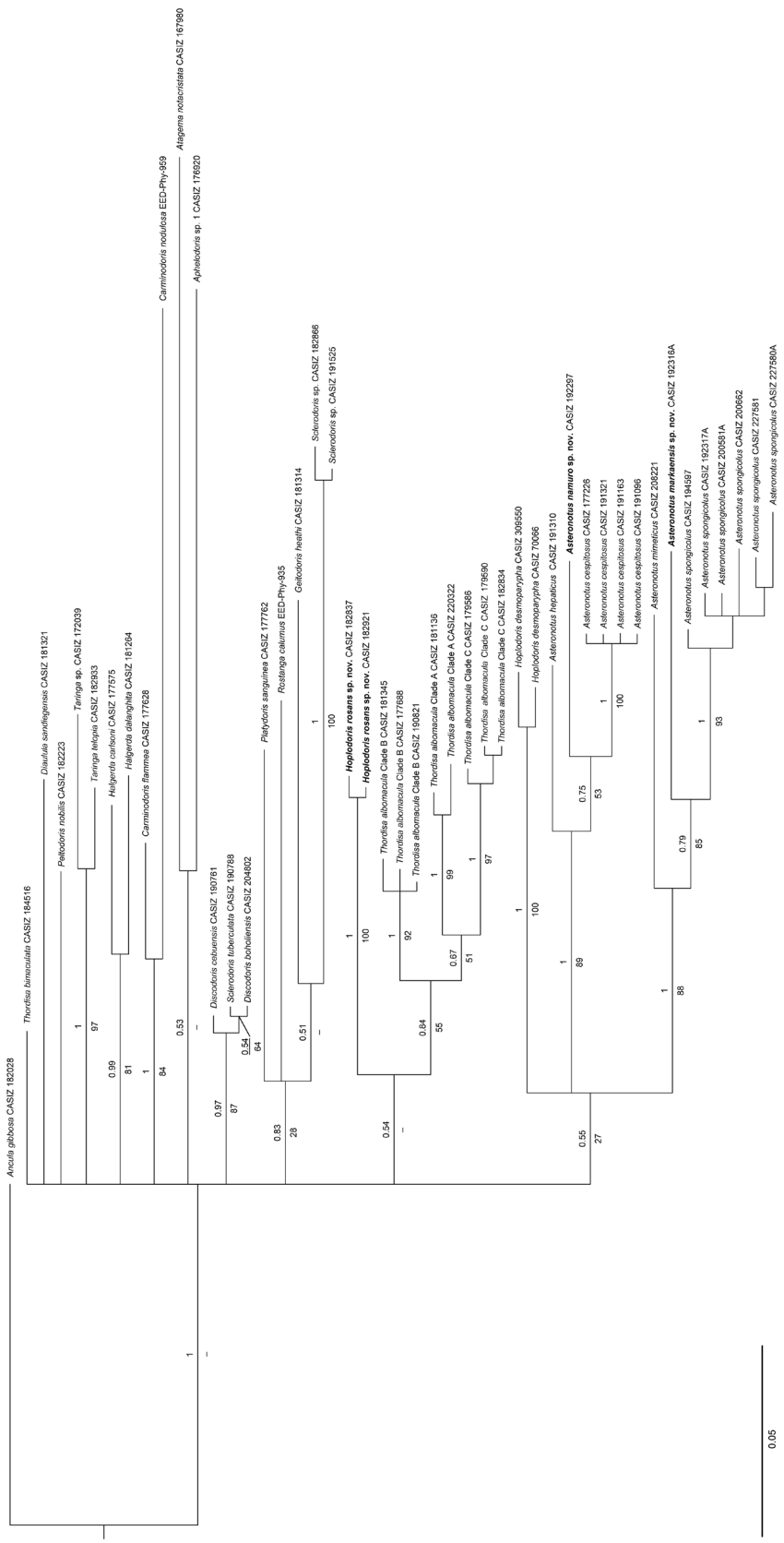

FIGURE S2. Phylogenetic tree estimated with Bayesian Inference (BI) and Maximum Likelihood (ML) for **16S**. Numbers above branches refer to BI posterior probabilities (pp), while numbers below branches refer to ML non-parametric bootstrapping values (bs). Relationships not recovered during ML analysis are indicated by dashes.

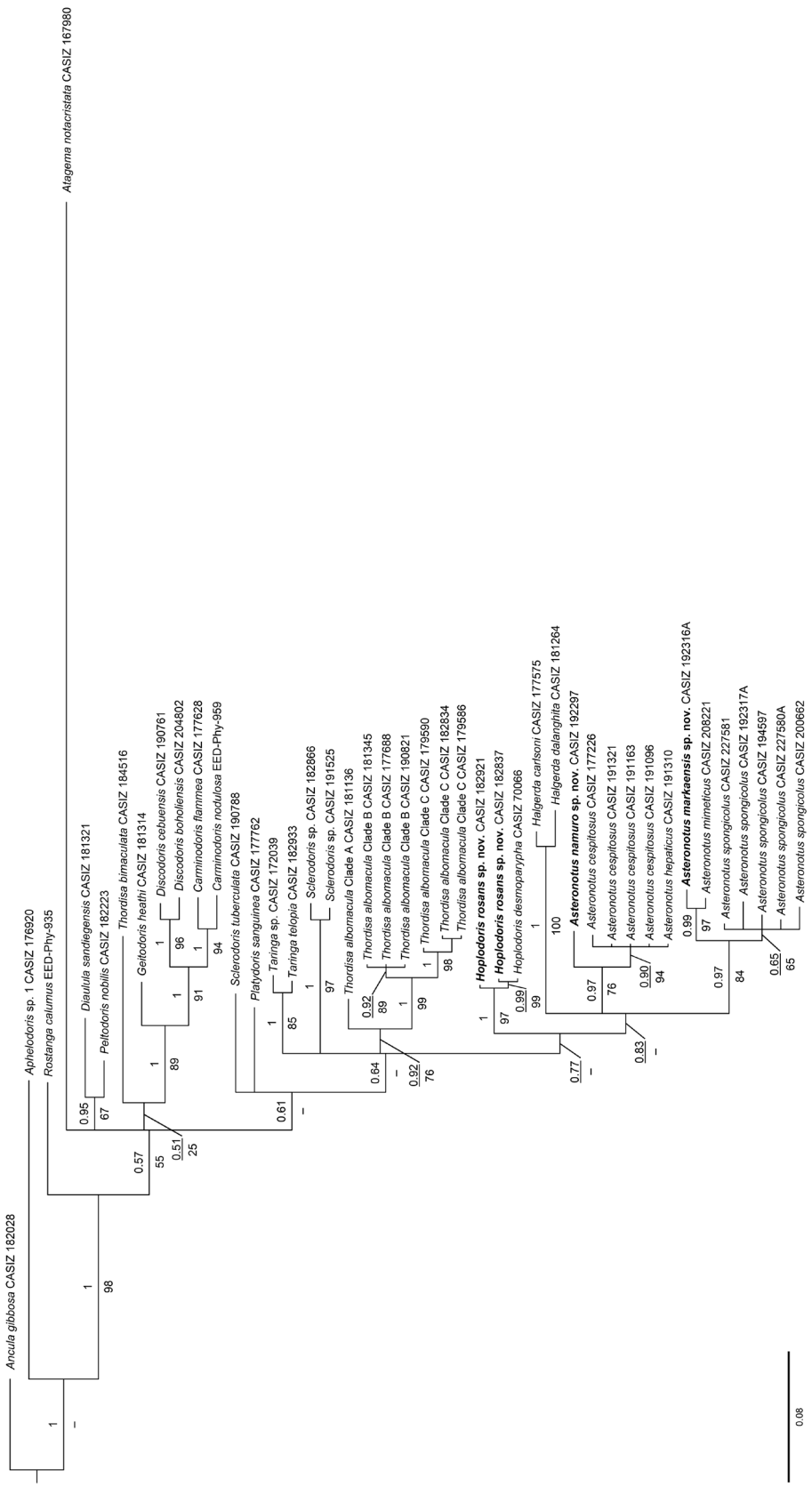

FIGURE S3. Phylogenetic tree estimated with Bayesian Inference (BI) and Maximum Likelihood (ML) for **28S**. Numbers above branches refer to BI posterior probabilities (pp), while numbers below branches refer to ML non-parametric bootstrapping values (bs). Relationships not recovered during ML analysis are indicated by dashes.

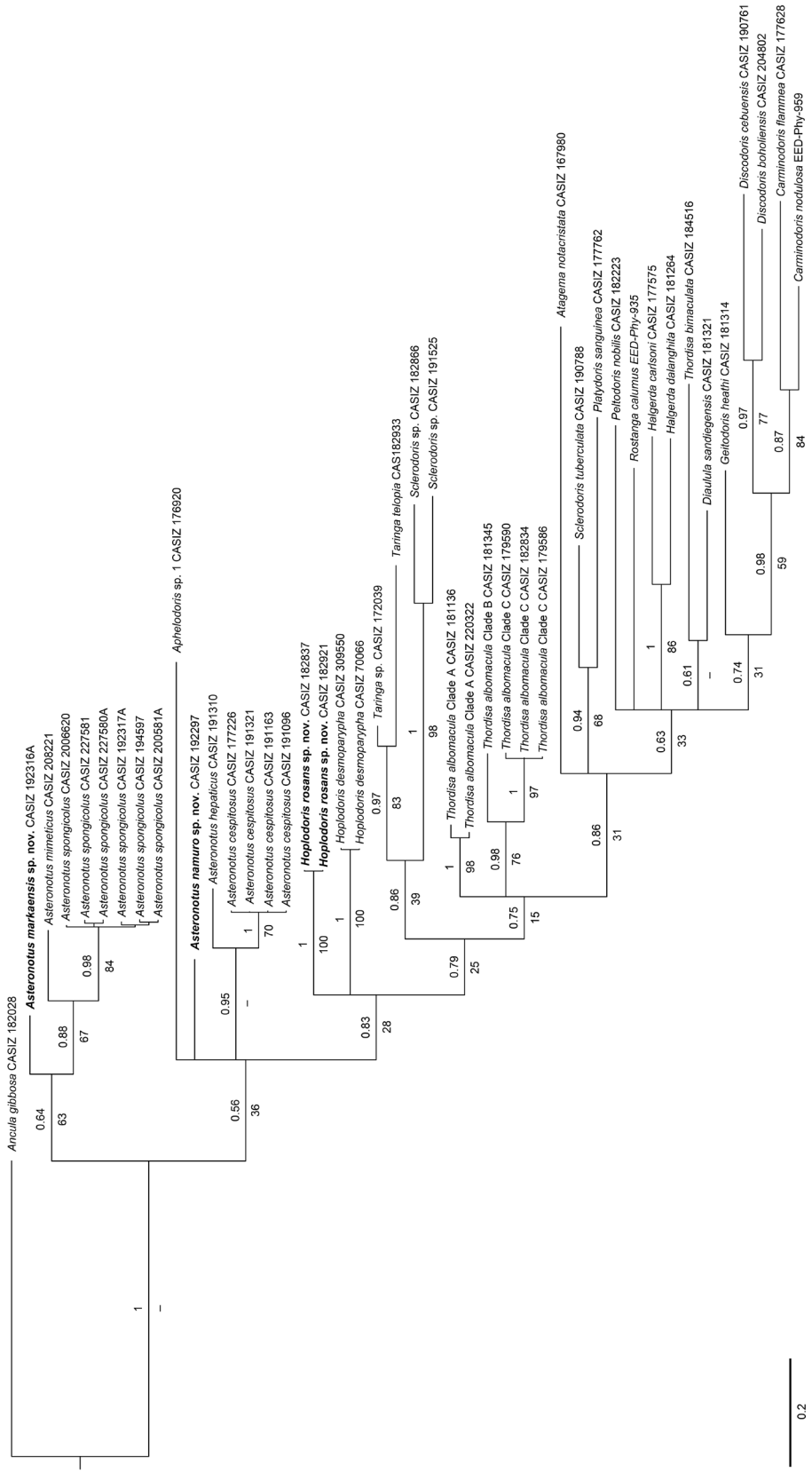

FIGURE S4. Phylogenetic tree estimated with Bayesian Inference (BI) and Maximum Likelihood (ML) for **COI**. Numbers above branches refer to BI posterior probabilities (pp), while numbers below branches refer to ML non-parametric bootstrapping values (bs). Relationships not recovered during ML analysis are indicated by dashes.

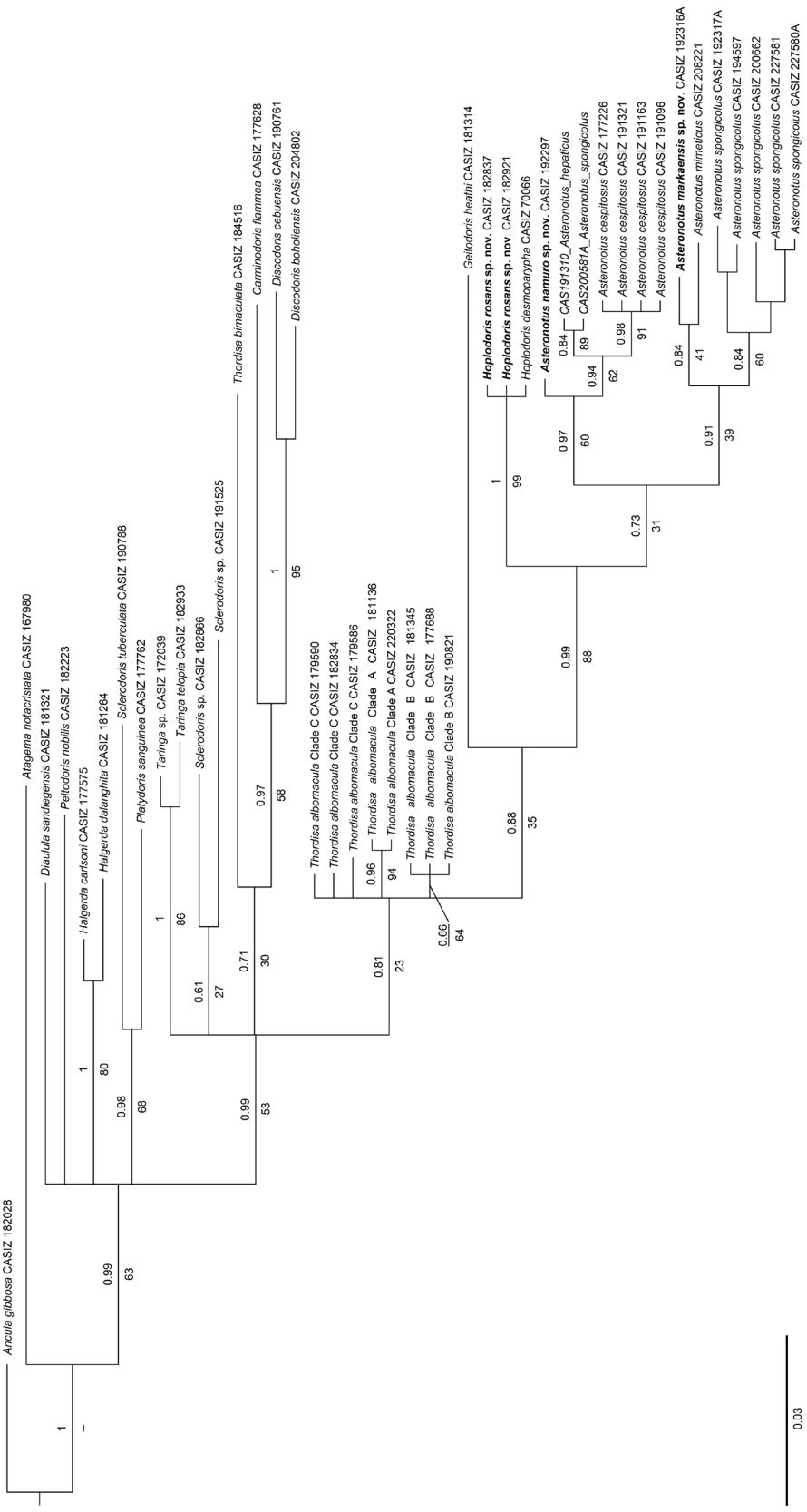

FIGURE S5. Phylogenetic tree estimated with Bayesian Inference (BI) and Maximum Likelihood (ML) for **H3**. Numbers above branches refer to BI posterior probabilities (pp), while numbers below branches refer to ML non-parametric bootstrapping values (bs). Relationships not recovered during ML analysis are indicated by dashes.

SUPPLEMENTARY TABLE 1. Primers for DNA amplification and Bayesian substitution models.

Primer	Sequence	Citation	Substitution Model	Length	
16S			GTR+I+G	453	
AR	5′-CGCCTGTTTATCAAAAACAT-3’	Palumbi *et al.* (1991)			
BR	5′-CCGGTCTGAACTCAGATCACGT-3’	Palumbi *et al.* (1991)			
28S			GTR+I+G	829	
D2	5’-CTTGGTCCGTGTTTCAAGACGG-3’	Dayrat *et al.* 2001 (modified)			
C1’	5’-ACCCGCTGAATTTAAGCAT-3’	Dayrat *et al.* (2001)			
C2’	5’-GAAAGAACTTTGAAGAGAGAGTTCA-3’	Dayrat *et al.* 2001 (modified)			
C2	5’-TGAACTCTCTCTTCAAAGTTCTTTTC-3’	Dayrat *et al.* (2001)			
Primer	Sequence	Citation	Substitution Model	Length	Codon Position
COI			HKY+G	220	P3
HCO2198	5′-TAAACTTCAGGGAGACCAAAAAATCA-3’	Folmer *et al.* (1994)	SYM+I+G	219	P1
LCO1490	5′-GGTCAACAAATCATAAAGATATTGG-3’	Folmer *et al.* (1994)	GTR+I+G	219	P2
H3			GTR+G	110	P1
AF	5’-ATGGCTCGTACCAAGCAGACVGC-3’	Colgan *et al.* (1998)	JC+I	110	P2
AR	5’-ATATCCTTRGGCATRATRGTGAC-3’	Colgan *et al.* (1998)	HKY+G	110	P3

SUPPLEMENTARY TABLE 2. PCR Protocols by primer set for 16S, 28S, COI, and H3 genetic markers.

Genetic Marker	16S		28S		COI		H3	
Primer Set	16SAR, 16SBR		D2, C2' & C1', C2		HCO2198, LCO1490		H3AF, H3AR	
PCR Phase	Temperature (°C)	Time (s)	Temperature (°C)	Time (s)	Temperature (°C)	Time (s)	Temperature (°C)	Time (s)
Initial Denaturation	94	180	95	240	94	180	94	180
Cycles	X40 of the Following		X40 of the Following		X40 of the Following		X35 of the Following	
Denaturation	94	30	94	30	94	30	94	30
Annealing	44–50	30	52.5	30	44–50	30	45–54	30
Extension	72	45	72	150	72	45	72	60
Followed By								
Final Extension	72	600	72	300	72	600	72	600